SUPPLEMENTAL MATERIAL FOR
Opposite-sign influences of canopy structural and physiological dynamics on water–carbon biogeography

Daniel Short Gianotti[1] and Dara Entekhabi[1]

[1]Parsons Laboratory for Environmental Science and Engineering, Department of Civil and Environmental Engineering, Massachusetts Institute of Technology, Cambridge, USA

Correspondence: Daniel Short Gianotti (gianotti@mit.edu)

1 Water–Productivity Literature Review

The study of spatial relationships (biogeography) between terrestrial productivity and climate dates to at least the mid-1700s (de Buffon, 1761; Forster, 1778; Hoorn et al., 2022). A central component of these relationships is the understanding that water availability exerts landscape-scale control on plant growth and productivity (Willdenow et al., 1805; Georg Forster, 1791; von Humboldt, 1807; Clements and Weaver, 1924; Humboldt and Bonpland, 2024; Green, 2024; Knapp et al., 2017), sometimes even when other variables are partially-limiting (Knapp et al., 2017; Feldman et al., 2018, 2021; Reich et al., 2025). This notion explicitly drives early bioclimate and agronomy classifications and foundational ecological theory (Wladimir Koppen, 1884; Koppen and Geiger, 1923; Lawes, 1848a, b; Clements, 1907; Clements and Weaver, 1924). Spatial biogeographical patterns have been broadly understood to be averaged or integrated responses to local temporal dynamics (Clements and Weaver, 1924; Goward and Prince, 1995; Azaele et al., 2006; Jin and Goulden, 2014; Reichstein et al., 2014), where fast processes like physiological regulation integrate to slower dynamics such as acclimation, population-scale adaptation, succession, homeostatic compensation, etc. (Lambers and Oliveira, 2019). These slow, integrated responses of landscape-scale vegetation dynamics to hydroclimate have been formalized into land-surface modeling efforts since their earliest days as spatial priors on vegetation characteristics and as prescribed water-limitation functions for primary productivity (Eagleson, 1978c, d, b; Lieth, 1975; Trugman et al., 2018).

1.1 Rain Use Efficiency: Spatial and Temporal Patterns

Because the linkages between daily-scale processes and successionary-or-longer processes are extremely difficult to constrain deterministically, various empirical relationships have been proposed to link water–productivity relationships across scales. The most intensely investigated is the rain-use efficiency relationship, typically linking monthly- or annual-scale precipitation and above-ground net productivity (RUE = P / ANPP), which has been studied in detail at individual sites and across sites (Walter, 1939; Currie and Peterson, 1966; Lauenroth, 1979; Houerou, 1980; Le Houerou, 1984). Early motivation for this relationship came as proposed linear relationships between ANPP and P over time at individual locations, and over space (as long-term

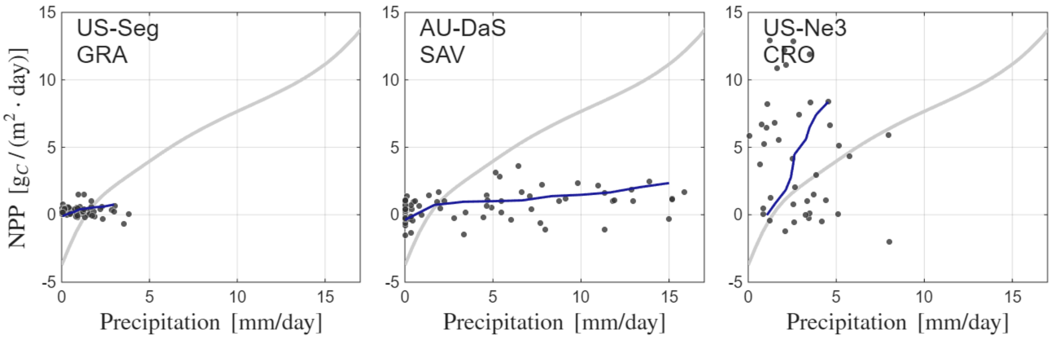

Fig. S1. Above-ground net primary productivity (ANPP) versus precipitation at monthly scale. Same as Main Text Figure 1a, but using ANPP in place GPP, both at landscape spatial scale (not scaled by f_v. This is the most commonly used form of the RUE relationship for local dynamics. Grey All-Sites curve is fit to all monthly growing season data from all 271 tower sites.

means) across locations (Hutchings, 1953; Sneva and Hyder, 1962; Rutherford, 1980; Smoliak, 1986; Le Houerou et al., 1988). The linear relationships were developed into empirical biogeographical models, at first suggesting a space-for-time convergence, but eventually seeming to show different temporal slopes in different hydroclimates, and a non-linear relationship across space (Sala et al., 1988; Noy-Meir, 1973; Lauenroth and Sala, 1992). There have since been many subsequent changes in framing (Hsu et al., 2012; Paruelo et al., 1999; Sala et al., 2012; Knapp et al., 2017), including accounting for the role of slow vegetation structural dynamics (Lauenroth and Sala, 1992; Knapp and Smith, 2001) and modified relationships in which biomes converge only under sufficient water stress (Huxman et al., 2004). Beyond the explicit RUE relationship, a number of similar resource-productivity ratios with water have been proposed (Nicholson et al., 1990; Farrar, 1991; Paruelo et al., 1999; Jin and Goulden, 2014), which tend to show a saturation or non-linearity as a function of seasonal, annual, or climatological precipitation.

1.2 Water-Use Efficiency and Evaporation

While precipitation was historically the most widely-measured water-cycle variable, plants respond to soil moisture and humidity mechanistically rather than precipitation itself (Wang et al., 2026), and other water fluxes such as evapotranspiration (ET) follow vegetation state variables better at their primary autocorrelation timescales (Eagleson, 1978c, d, e, b; Short Giantotti et al., 2020; Feldman, 2025; Teuling et al., 2006; McColl et al., 2017; Feldman et al., 2018; Sehgal et al., 2021; Holtzman et al., 2024). This, along with chamber-scale gas-exchange studies, have led to measurements and models of productivity as a function of ET rather than precipitation, with the relationship or the ratio typically termed landscape- or ecosystem-water-use efficiency (WUE) (Mikhail I Budyko, 1971; Rosenzweig, 1968). WUE and ET have also served as climate classification variables (Livingston, 1906; Briggs and Shantz, 1913; Maximow and Krasnosselsky-Maximow, 1924; Clements, 1920; Huang et al., 2016; Mu et al., 2013; Thornthwaite, 1948), and both an indicator of water availability and a product of plant productivity itself. Recent observational work has sought to generalize productivity–ET relationships by building on RUE relationships (Biederman et al., 2016; Scott et al., 2015), through direct comparison (Garbulsky et al., 2010; Yang et al., 2016; Huang et al., 2016; Short Gianotti et al., 2019), and as the basis for global remotely-sensed products (Mu et al., 2013, 2007), although the relationships have been shown to vary widely across climate conditions (Short Gianotti et al., 2019; Yu et al., 2008; Cheng et al., 2017; Sun et al., 2016).

1.2.1 Evaporative Fraction as Water Metric

More recently, Short Gianotti and Entekhabi (2024) demonstrated a water–productivity relationship which does show the same temporal and spatial relationship, namely the relationship between evaporative fraction (EF) and GPP ($\mathrm{EF} = \mathrm{L}\cdot\mathrm{ET}/\mathrm{A}$, where A is available energy and L is the latent heat of vaporization for water, see Table 1). They demonstrated that GPP–EF relationships at monthly timescales follow a similar convergent relationship across biogeography and climate at a large number of eddy covariance tower sites (Short Gianotti and Entekhabi, 2024), and proposed that this single empirical functional relationship may describe coupling across both space and time, with the spatial relationship emerging as an artifact of convergent temporal relationships across sites. Using EF rather than ET controls for surface energy budget effects on moisture flux magnitudes and energy-limitation, leading to more convergent relationships with volumetric soil moisture (Short Gianotti et al., 2019; Dirmeyer et al., 2000) and the atmospheric boundary layer (Hay-Chapman and Dirmeyer, 2023) across latitude and climate gradients. Like the RUE relationship, this GPP–EF relationship is non-linear, and so cannot converge to a single time and space relation across different aggregation timescale without transformation (i.e., due to Jenson's inequality, Short Gianotti and Entekhabi, 2024), but unlike the RUE relationship, local monthly dynamics are tangent to the general monthly relationship across all sites (Knapp et al., 2017; Short Gianotti et al., 2024).

Short Gianotti et al. (2024) identify two dominant timescales in the between-storm component of the GPP–EF functional relationship: a fast rain-pulse timescale of 3–5 days, and a slower relaxation timescale of roughly 3-5 weeks. Critically, these timescales show opposing relationships; water and carbon are negatively correlated at fast timescales (increased uptake while drying) but positively correlated at slower timescales (decreased uptake while drying). They hypothesize that the dynamics of canopy fractional cover (f_v) or LAI might link these timescales as an integrator of responses to weather-scale events.

2 Transpiration Intensity Ratio

In the manuscript we invoke the variable

$$\phi = \frac{T_c}{ET_l} = \frac{1}{f_v}\frac{T_l}{ET_l} \qquad \text{(Main Text 3)}$$

where T_c is the (intensive) transpiration rate averaged over just the canopy area, ET_l is the landscape-averaged evapotranspiration rate (total water volume evaporated per time divided by the full landscape area), f_v is the vegetation cover fraction, T_l is the transpiration rate if averaged over the total landscape (bare soil and canopy) area, and T_l/ET_l is the commonly-referenced "T over ET ratio." To be even more specific, if evaporation is comprised only of soil evaporation E_s over an un-vegetated area fraction $1 - f_v$, and transpiration over a vegetated area f_v, we could write the landscape ET as

$$ET_l = f_v T_c + (1 - f_v) E_s \tag{S1}$$

Using the basic Fick's law form of the evaporation rate,

$$ET_l = f_v \cdot \underbrace{\rho \frac{g_c g_{a,c}}{g_c + g_{a,c}} \left[q^\star(\theta_c) - q_c\right]}_{T_c} + (1 - f_v) \cdot \underbrace{\rho \frac{g_s g_{a,s}}{g_s + g_{a,s}} \left[q^\star(\theta_s) - q_s\right]}_{E_s} \tag{S2}$$

where ρ is the density of the atmosphere at the land surface [kg/m^3], g_c is the canopy-averaged conductance for water vapor [m/s] from saturated air within leaves at leaf temperatures θ_c, $g_{a,c}$ is the aerodynamic conductance above the canopy [m/s], $q^\star$ is the saturation specific vapor pressure for a given air temperature [$-$], q_c is the specific humidity above the canopy [$-$], g_s is the bare soil-averaged conductance for water vapor [m/s] from saturated air within soil pores at skin temperature θ_s, $g_{a,s}$ is the aerodynamic conductance above the bare soil portion of the landscape, and q_s is the specific humidity above the bare soil portion of the landscape [$-$]. Note that this is a "big leaf" and "big soil pore" model of evaporation where the conductances are intended to represent some bulk properties of the heterogeneous vegetated and bare portions of the landscape.

Under the common modeling practice of having single air temperatures, humidities, wind speed distributions, and skin temperatures within a grid cell, this would be simplified to

$$ET_l = \rho g_a \left[q^\star(\theta_{surf}) - q\right] \left[f_v \frac{g_c}{g_c + g_a} + (1 - f_v) \frac{g_s}{g_s + g_a}\right] \tag{S3}$$

and ϕ itself can then be written as the ratio of the bulk conductance over the canopy to the bulk conductance over the entire landscape:

$$\phi = \frac{\frac{g_a g_c}{g_a + g_c}}{f_v \frac{g_a g_c}{g_a + g_c} + (1 - f_v) \frac{g_a g_s}{g_a + g_s}} = \frac{g_c (g_s + g_a)}{g_s (g_c + g_a) + f_v g_a (g_c - g_s)} \tag{S4}$$

When intensive soil and canopy conductances are equal, $g_s = g_c$, then $\phi = 1$. When bare soil evaporation is zero and $g_s = 0$, $\phi = \frac{1}{f_v} \geq 1$, and when canopy conductance is zero, $\phi = 0$.

Fully separating the dynamics of ω_c and ϕ requires separation of transpiration from bare soil evaporation observationally. There is opportunity to investigate this at co-located Eddy Covariance Flux Tower sites and SapFlux observation sties (Poyatos et al., 2016), provided there is sufficient understanding of spatial vegetation scaling, tower footprint dynamics, moisture availability, humidity heterogeneity, and temperature heterogeneity.

Because neither ϕ nor ω_c are commonly measured, we perform our analyses using their product $\omega_c \phi$, which is calculated at daily scale as the residual of the other observed terms, $GPP_l/(f_v ET_l)$, in grams carbon per gram of water. If bare soils and vegetation respond similarly to changes in soil moisture and vapor pressure deficit (VPD), then $\phi = 1$, and this is exactly the canopy WUE, ω_c. ϕ, the ratio of transpiration intensity to total ET intensity (which can be written primarily in terms of conductances), is sometimes referred to as the "plant coefficient," and though its dynamics are not well-studied globally, it has been argued to be relatively constant locally, due to similar bare soil and transpiration responses to water limitation, across the growing season and during inter-storm drydowns (Eagleson, 1978c, e; Sellers et al., 1997; Ács, 2003). The largest variability appears to be climatic across space (Eagleson, 1978a; Unkovich et al., 2018); if this is true, then $\omega_c\phi$ dynamics can be interpreted simply as scaled ω_c dynamics. We do not have sufficient data with which to validate this claim, and leave the relationship between $\omega_c\phi$ and the standard canopy water-use efficiency ω_c open to reader interpretation.

3 Flux Tower Variables

The primary data in this study come from measurements made at flux towers using eddy covariance methods to estimate exchanges of energy and mass between the atmosphere, the land surface, and terrestrial biota. In recent decades, many science teams operating these tower sites have coordinated to standardize and disseminate their data for public use (Baldocchi et al., 2001; Novick et al., 2018; Pastorello et al., 2020; Chu et al., 2023); we draw from two of these major data networks for this study: (1) the FLUXNET network, and (2) the AmeriFlux network. From FLUXNET, we use data from the FLUXNET 2015 data release (Pastorello et al., 2020). From the AmeriFlux network we use data from both of the AmeriFlux BASE dataset and the AmeriFlux FLUXNET SUBSET dataset (Boden et al., 2013; Pastorello et al., 2020; Chu et al., 2023). From all datasets we use all site data released under the CC-by-4.0 license. For sites appearing in multiple datasets, we select the record with the longest available data period. Specifics for each tower site are presented in Supplemental Table 1, and citations for each site's data are in Supplemental Section 6.

3.1 Excluded sites

For all analyses, we exclude sites with landcover classifications of open water, wetland, or snow and ice. None of the data meeting our criteria are classified as urban or barren. Throughout the analyses, we define *growing season months* for each tower as those calendar months with GPP greater than or equal to 10% of the maximum monthly GPP in that site's data record. All following analyses use only data from growing season months.

3.2 Variables used

For each AmeriFlux or FLUXNET site record, we extract daily values of the following: latent heat flux (LE_F_MDS), sensible heat flux (H_F_MDS), precipitation (P_F_MDS), and gross primary productivity using the nighttime respiration partitioning method (GPP_NT_VUT_REF). When daily data are not available, we aggregate hourly or half-hourly data to daily. Only days with at least 22 of 24 hourly or 44 of 48 hourly-hourly observations are used. Missing hourly or half-hourly data are replaced with the monthly-averaged value of the variable for the corresponding time-of-day to avoid sampling biases.

From the turbulent fluxes (latent and sensible), we calculate daily and monthly values of the evaporative fraction, $EF = LE/(H+LE)$. Monthly evaporative fraction is calculated as $EF = \Sigma\ \mathrm{LE}/(\Sigma\ \mathrm{LE} + \Sigma\ \mathrm{H})$, adding over all days prior to division. We use EF throughout the analyses as an energy-normalized evaporative flux. By dividing by available turbulent energy ($H + LE$, equal to net radiation minus ground heat flux), we are able to control to some extent for latitudinal and weather-driven differences in temperature and radiation, and can focus on the water and carbon variables without the covarying influence of the surface energy budget as well. EF and GPP have been investigated together (Short Gianotti et al., 2019; Short Gianotti and Entekhabi, 2024; Short Gianotti et al., 2024), and have shown empirical spatial and temporal coupling which these analyses aim to explain mechanistically.

4 Table of Flux Tower Info

Site ID	Source	Years	Months	IGBP	Lat.	Lon.	Dataset DOI
CA-Ca1	AmeriFlux BASE	1996-2010	86	ENF	49.867	-125.334	https://doi.org/10.17190/AMF/1480300
CA-Ca2	AmeriFlux BASE	1999-2010	41	ENF	49.871	-125.291	https://doi.org/10.17190/AMF/1480301
CA-Ca3	AmeriFlux BASE	2001-2022	65	ENF	49.535	-124.9	https://doi.org/10.17190/AMF/1480302
CA-LP1	AmeriFlux BASE	2007-2022	71	ENF	55.112	-122.841	https://doi.org/10.17190/AMF/1660337
CA-TP1	AmeriFlux BASE	2002-2017	61	ENF	42.661	-80.56	https://doi.org/10.17190/AMF/1246009
CA-TP4	AmeriFlux BASE	2002-2017	86	ENF	42.71	-80.357	https://doi.org/10.17190/AMF/1246012
US-Bi1	AmeriFlux BASE	2016-2023	56	CRO	38.099	-121.499	https://doi.org/10.17190/AMF/1480317
US-CMW	AmeriFlux BASE	2000-2021	122	DBF	31.664	-110.178	https://doi.org/10.17190/AMF/1660339
US-EML	AmeriFlux BASE	2008-2020	46	OSH	63.878	-149.254	https://doi.org/10.17190/AMF/1418678
US-ICh	AmeriFlux BASE	2007-2021	40	OSH	68.607	-149.296	https://doi.org/10.17190/AMF/1246133
US-Kon	AmeriFlux BASE	2004-2019	21	GRA	39.082	-96.56	https://doi.org/10.17190/AMF/1246068
US-LL1	AmeriFlux BASE	2009-2020	136	SAV	31.279	-84.533	https://doi.org/10.17190/AMF/1773395
US-LL2	AmeriFlux BASE	2009-2017	101	SAV	31.201	-84.445	https://doi.org/10.17190/AMF/1773396
US-LL3	AmeriFlux BASE	2009-2017	104	SAV	31.269	-84.479	https://doi.org/10.17190/AMF/1773397
US-LS1	AmeriFlux BASE	2002-2007	28	GRA	31.562	-110.14	https://doi.org/10.17190/AMF/1660346
US-LS2	AmeriFlux BASE	2002-2007	30	SAV	31.566	-110.134	https://doi.org/10.17190/AMF/1660347
US-Me2	AmeriFlux BASE	2002-2022	123	ENF	44.452	-121.557	https://doi.org/10.17190/AMF/1246076
US-Ne2	AmeriFlux BASE	2001-2020	25	CRO	41.165	-96.47	https://doi.org/10.17190/AMF/1246085
US-Ne3	AmeriFlux BASE	2001-2020	33	CRO	41.18	-96.44	https://doi.org/10.17190/AMF/1246086
US-PFa	AmeriFlux BASE	1995-2023	93	MF	45.946	-90.272	https://doi.org/10.17190/AMF/1246090
US-Prr	AmeriFlux BASE	2010-2016	25	ENF	65.124	-147.488	https://doi.org/10.17190/AMF/1246153
US-Rpf	AmeriFlux BASE	2008-2022	37	DBF	65.12	-147.429	https://doi.org/10.17190/AMF/1579540
US-Syv	AmeriFlux BASE	2001-2023	56	MF	46.242	-89.348	https://doi.org/10.17190/AMF/1246106
US-Ton	AmeriFlux BASE	2001-2022	130	WSA	38.431	-120.966	https://doi.org/10.17190/AMF/1245971
US-Uaf	AmeriFlux BASE	2003-2022	79	ENF	64.866	-147.856	https://doi.org/10.17190/AMF/1480322
US-Var	AmeriFlux BASE	2000-2022	82	GRA	38.413	-120.951	https://doi.org/10.17190/AMF/1245984
US-WCr	AmeriFlux BASE	1998-2023	33	DBF	45.806	-90.08	https://doi.org/10.17190/AMF/1246111
BR-Npw	AmeriFlux FLUXNET	2013-2017	52	WSA	-16.498	-56.412	https://doi.org/10.17190/AMF/1579716

CA-Cbo	AmeriFlux FLUXNET	1994-2020	103	DBF	44.317	-79.933	https://doi.org/10.17190/AMF/1498755
CA-TP3	AmeriFlux FLUXNET	2002-2017	70	ENF	42.707	-80.348	https://doi.org/10.17190/AMF/1246011
CA-TPD	AmeriFlux FLUXNET	2012-2017	30	DBF	42.635	-80.558	https://doi.org/10.17190/AMF/1246152
US-ARM	AmeriFlux FLUXNET	2003-2020	58	CRO	36.606	-97.489	https://doi.org/10.17190/AMF/1246027
US-BZS	AmeriFlux FLUXNET	2010-2021	40	ENF	64.696	-148.324	https://doi.org/10.17190/AMF/1756434
US-GLE	AmeriFlux FLUXNET	2005-2020	69	ENF	41.367	-106.24	https://doi.org/10.17190/AMF/1246056
US-Ha1	AmeriFlux FLUXNET	1991-2020	131	DBF	42.538	-72.172	https://doi.org/10.17190/AMF/1246059
US-Ho2	AmeriFlux FLUXNET	1999-2020	86	ENF	45.209	-68.747	https://doi.org/10.17190/AMF/1246062
US-Jo1	AmeriFlux FLUXNET	2010-2020	61	OSH	32.582	-106.635	https://doi.org/10.17190/AMF/1767833
US-Jo2	AmeriFlux FLUXNET	2010-2020	60	OSH	32.585	-106.603	https://doi.org/10.17190/AMF/1617696
US-KFS	AmeriFlux FLUXNET	2007-2019	49	GRA	39.056	-95.191	https://doi.org/10.17190/AMF/1246132
US-KLS	AmeriFlux FLUXNET	2012-2019	36	GRA	38.775	-97.568	https://doi.org/10.17190/AMF/1498745
US-MMS	AmeriFlux FLUXNET	1999-2020	114	DBF	39.323	-86.413	https://doi.org/10.17190/AMF/1246080
US-MOz	AmeriFlux FLUXNET	2004-2019	70	DBF	38.744	-92.2	https://doi.org/10.17190/AMF/1246081
US-Mpj	AmeriFlux FLUXNET	2008-2020	122	OSH	34.438	-106.238	https://doi.org/10.17190/AMF/1246123
US-NC1	AmeriFlux FLUXNET	2005-2012	53	OSH	35.812	-76.712	https://doi.org/10.17190/AMF/1246082
US-NR1	AmeriFlux FLUXNET	1998-2016	84	ENF	40.033	-105.546	https://doi.org/10.17190/AMF/1246088
US-Ne1	AmeriFlux FLUXNET	2001-2020	58	CRO	41.165	-96.477	https://doi.org/10.17190/AMF/1246084
US-ONA	AmeriFlux FLUXNET	2015-2020	52	GRA	27.384	-81.951	https://doi.org/10.17190/AMF/1660350
US-Rms	AmeriFlux FLUXNET	2014-2020	28	CSH	43.065	-116.749	https://doi.org/10.17190/AMF/1375202
US-Ro1	AmeriFlux FLUXNET	2004-2016	24	CRO	44.714	-93.09	https://doi.org/10.17190/AMF/1246092
US-Rwe	AmeriFlux FLUXNET	2003-2007	20	CSH	43.065	-116.759	https://doi.org/10.17190/AMF/1617721
US-Rwf	AmeriFlux FLUXNET	2014-2020	24	CSH	43.121	-116.723	https://doi.org/10.17190/AMF/1617724
US-Rws	AmeriFlux FLUXNET	2014-2020	31	OSH	43.168	-116.713	https://doi.org/10.17190/AMF/1375201
US-Seg	AmeriFlux FLUXNET	2007-2021	43	GRA	34.362	-106.702	https://doi.org/10.17190/AMF/1246124
US-Ses	AmeriFlux FLUXNET	2007-2021	48	OSH	34.335	-106.744	https://doi.org/10.17190/AMF/1246125
US-Sne	AmeriFlux FLUXNET	2016-2020	20	GRA	38.037	-121.755	https://doi.org/10.17190/AMF/1418684
US-Tw3	AmeriFlux FLUXNET	2013-2018	39	CRO	38.115	-121.647	https://doi.org/10.17190/AMF/1246149

US-UMd	AmeriFlux FLUXNET	2007-2021	63	DBF	45.563	-84.698	https://doi.org/10.17190/AMF/1246134
US-Whs	AmeriFlux FLUXNET	2007-2020	28	OSH	31.744	-110.052	https://doi.org/10.17190/AMF/1246113
US-Wjs	AmeriFlux FLUXNET	2007-2021	96	SAV	34.426	-105.862	https://doi.org/10.17190/AMF/1246120
US-Wkg	AmeriFlux FLUXNET	2004-2021	49	GRA	31.737	-109.942	https://doi.org/10.17190/AMF/1246112
US-xBR	AmeriFlux FLUXNET	2017-2021	25	DBF	44.064	-71.287	https://doi.org/10.17190/AMF/1579542
US-xDS	AmeriFlux FLUXNET	2017-2021	28	CVM	28.125	-81.436	https://doi.org/10.17190/AMF/1671895
US-xHA	AmeriFlux FLUXNET	2017-2021	25	DBF	42.537	-72.173	https://doi.org/10.17190/AMF/1562391
US-xJE	AmeriFlux FLUXNET	2017-2021	22	ENF	31.195	-84.469	https://doi.org/10.17190/AMF/1617730
US-xSB	AmeriFlux FLUXNET	2017-2021	28	ENF	29.689	-81.993	https://doi.org/10.17190/AMF/1671899
US-xTA	AmeriFlux FLUXNET	2017-2021	33	ENF	32.951	-87.393	https://doi.org/10.17190/AMF/1671902
US-xTR	AmeriFlux FLUXNET	2017-2021	20	DBF	45.494	-89.586	https://doi.org/10.17190/AMF/1634886
US-xUN	AmeriFlux FLUXNET	2017-2021	20	MF	46.234	-89.537	https://doi.org/10.17190/AMF/1617741
AT-Neu	Fluxnet 2015	2002-2012	65	GRA	47.117	11.318	https://doi.org/10.18140/FLX/1440121
AU-Cpr	Fluxnet 2015	2010-2014	39	SAV	-34.002	140.589	https://doi.org/10.18140/FLX/1440195
AU-Cum	Fluxnet 2015	2012-2014	24	EBF	-33.615	150.724	https://doi.org/10.18140/FLX/1440196
AU-DaP	Fluxnet 2015	2007-2013	29	GRA	-14.063	131.318	https://doi.org/10.18140/FLX/1440123
AU-DaS	Fluxnet 2015	2008-2014	65	SAV	-14.159	131.388	https://doi.org/10.18140/FLX/1440122
AU-Dry	Fluxnet 2015	2008-2014	48	SAV	-15.259	132.371	https://doi.org/10.18140/FLX/1440197
AU-GWW	Fluxnet 2015	2013-2014	23	SAV	-30.191	120.654	https://doi.org/10.18140/FLX/1440200
AU-Gin	Fluxnet 2015	2011-2014	33	WSA	-31.376	115.714	https://doi.org/10.18140/FLX/1440199
AU-How	Fluxnet 2015	2001-2014	127	WSA	-12.494	131.152	https://doi.org/10.18140/FLX/1440125
AU-Rig	Fluxnet 2015	2011-2014	20	GRA	-36.65	145.576	https://doi.org/10.18140/FLX/1440202
AU-Stp	Fluxnet 2015	2008-2014	27	GRA	-17.151	133.35	https://doi.org/10.18140/FLX/1440204
AU-Tum	Fluxnet 2015	2001-2014	134	EBF	-35.657	148.152	https://doi.org/10.18140/FLX/1440126
AU-Wac	Fluxnet 2015	2005-2008	21	EBF	-37.426	145.188	https://doi.org/10.18140/FLX/1440127
AU-Whr	Fluxnet 2015	2011-2014	36	EBF	-36.673	145.029	https://doi.org/10.18140/FLX/1440206
AU-Wom	Fluxnet 2015	2010-2014	39	EBF	-37.422	144.094	https://doi.org/10.18140/FLX/1440207
BE-Bra	Fluxnet 2015	1996-2014	94	MF	51.308	4.52	https://doi.org/10.18140/FLX/1440128

BE-Lon	Fluxnet 2015	2004-2014	31	CRO	50.552	4.746	https://doi.org/10.18140/FLX/1440129
BE-Vie	Fluxnet 2015	1996-2014	123	MF	50.305	5.998	https://doi.org/10.18140/FLX/1440130
BR-Sa1	Fluxnet 2015	2002-2011	90	EBF	-2.857	-54.959	https://doi.org/10.18140/FLX/1440032
BR-Sa3	Fluxnet 2015	2000-2004	44	EBF	-3.018	-54.971	https://doi.org/10.18140/FLX/1440033
CA-Gro	Fluxnet 2015	2003-2014	50	MF	48.217	-82.156	https://doi.org/10.18140/FLX/1440034
CA-Man	Fluxnet 2015	1994-2008	62	ENF	55.88	-98.481	https://doi.org/10.18140/FLX/1440035
CA-NS2	Fluxnet 2015	2001-2005	21	ENF	55.906	-98.525	https://doi.org/10.18140/FLX/1440037
CA-NS3	Fluxnet 2015	2001-2005	21	ENF	55.912	-98.382	https://doi.org/10.18140/FLX/1440038
CA-Oas	Fluxnet 2015	1996-2010	60	DBF	53.629	-106.198	https://doi.org/10.18140/FLX/1440043
CA-Obs	Fluxnet 2015	1997-2010	62	ENF	53.987	-105.118	https://doi.org/10.18140/FLX/1440044
CA-Qfo	Fluxnet 2015	2003-2010	33	ENF	49.693	-74.342	https://doi.org/10.18140/FLX/1440045
CA-SF1	Fluxnet 2015	2003-2006	26	ENF	54.485	-105.818	https://doi.org/10.18140/FLX/1440046
CA-SF2	Fluxnet 2015	2001-2005	25	ENF	54.254	-105.878	https://doi.org/10.18140/FLX/1440047
CA-SF3	Fluxnet 2015	2001-2006	28	OSH	54.092	-106.005	https://doi.org/10.18140/FLX/1440048
CH-Cha	Fluxnet 2015	2005-2014	66	GRA	47.21	8.41	https://doi.org/10.18140/FLX/1440131
CH-Dav	Fluxnet 2015	1997-2014	113	ENF	46.815	9.856	https://doi.org/10.18140/FLX/1440132
CH-Fru	Fluxnet 2015	2005-2014	61	GRA	47.116	8.538	https://doi.org/10.18140/FLX/1440133
CH-Lae	Fluxnet 2015	2004-2014	65	MF	47.478	8.364	https://doi.org/10.18140/FLX/1440134
CH-Oe1	Fluxnet 2015	2002-2008	42	GRA	47.286	7.732	https://doi.org/10.18140/FLX/1440135
CH-Oe2	Fluxnet 2015	2004-2014	37	CRO	47.286	7.734	https://doi.org/10.18140/FLX/1440136
CN-Din	Fluxnet 2015	2003-2005	34	EBF	23.173	112.536	https://doi.org/10.18140/FLX/1440139
CN-Qia	Fluxnet 2015	2003-2005	32	ENF	26.741	115.058	https://doi.org/10.18140/FLX/1440141
CZ-BK1	Fluxnet 2015	2004-2014	84	ENF	49.502	18.537	https://doi.org/10.18140/FLX/1440143
CZ-BK2	Fluxnet 2015	2004-2012	37	GRA	49.494	18.543	https://doi.org/10.18140/FLX/1440144
DE-Geb	Fluxnet 2015	2001-2014	42	CRO	51.1	10.915	https://doi.org/10.18140/FLX/1440146
DE-Gri	Fluxnet 2015	2004-2014	66	GRA	50.95	13.513	https://doi.org/10.18140/FLX/1440147
DE-Hai	Fluxnet 2015	2000-2012	49	DBF	51.079	10.452	https://doi.org/10.18140/FLX/1440148
DE-Kli	Fluxnet 2015	2004-2014	31	CRO	50.893	13.522	https://doi.org/10.18140/FLX/1440149

DE-Lkb	Fluxnet 2015	2009-2013	21	ENF	49.1	13.305	https://doi.org/10.18140/FLX/1440214
DE-Lnf	Fluxnet 2015	2002-2012	39	DBF	51.328	10.368	https://doi.org/10.18140/FLX/1440150
DE-Obe	Fluxnet 2015	2008-2014	44	ENF	50.787	13.721	https://doi.org/10.18140/FLX/1440151
DE-RuR	Fluxnet 2015	2011-2014	25	GRA	50.622	6.304	https://doi.org/10.18140/FLX/1440215
DE-Tha	Fluxnet 2015	1996-2014	122	ENF	50.963	13.565	https://doi.org/10.18140/FLX/1440152
DK-Sor	Fluxnet 2015	1996-2014	74	DBF	55.486	11.645	https://doi.org/10.18140/FLX/1440155
ES-Amo	Fluxnet 2015	2007-2012	21	OSH	36.834	-2.252	https://doi.org/10.18140/FLX/1440156
ES-LJu	Fluxnet 2015	2004-2013	28	OSH	36.927	-2.752	https://doi.org/10.18140/FLX/1440157
FI-Hyy	Fluxnet 2015	1996-2014	93	ENF	61.847	24.295	https://doi.org/10.18140/FLX/1440158
FI-Sod	Fluxnet 2015	2001-2014	61	ENF	67.362	26.639	https://doi.org/10.18140/FLX/1440160
FR-Fon	Fluxnet 2015	2005-2014	49	DBF	48.476	2.78	https://doi.org/10.18140/FLX/1440161
FR-Gri	Fluxnet 2015	2004-2014	28	CRO	48.844	1.952	https://doi.org/10.18140/FLX/1440162
FR-LBr	Fluxnet 2015	1996-2008	83	ENF	44.717	-0.769	https://doi.org/10.18140/FLX/1440163
FR-Pue	Fluxnet 2015	2000-2014	103	EBF	43.741	3.596	https://doi.org/10.18140/FLX/1440164
GF-Guy	Fluxnet 2015	2004-2014	119	EBF	5.279	-52.925	https://doi.org/10.18140/FLX/1440165
GH-Ank	Fluxnet 2015	2011-2014	24	EBF	5.269	-2.694	https://doi.org/10.18140/FLX/1440229
GL-ZaH	Fluxnet 2015	2000-2014	28	GRA	74.473	-20.55	https://doi.org/10.18140/FLX/1440224
IT-BCi	Fluxnet 2015	2004-2014	43	CRO	40.524	14.957	https://doi.org/10.18140/FLX/1440166
IT-Col	Fluxnet 2015	1996-2014	75	DBF	41.849	13.588	https://doi.org/10.18140/FLX/1440167
IT-Cpz	Fluxnet 2015	1997-2009	68	EBF	41.705	12.376	https://doi.org/10.18140/FLX/1440168
IT-Lav	Fluxnet 2015	2003-2014	96	ENF	45.956	11.281	https://doi.org/10.18140/FLX/1440169
IT-MBo	Fluxnet 2015	2003-2013	59	GRA	46.015	11.046	https://doi.org/10.18140/FLX/1440170
IT-Noe	Fluxnet 2015	2004-2014	82	CSH	40.606	8.152	https://doi.org/10.18140/FLX/1440171
IT-Ren	Fluxnet 2015	1998-2013	77	ENF	46.587	11.434	https://doi.org/10.18140/FLX/1440173
IT-Ro1	Fluxnet 2015	2000-2008	51	DBF	42.408	11.93	https://doi.org/10.18140/FLX/1440174
IT-Ro2	Fluxnet 2015	2002-2012	56	DBF	42.39	11.921	https://doi.org/10.18140/FLX/1440175
IT-SRo	Fluxnet 2015	1999-2012	102	ENF	43.728	10.284	https://doi.org/10.18140/FLX/1440176
IT-Tor	Fluxnet 2015	2008-2014	27	GRA	45.844	7.578	https://doi.org/10.18140/FLX/1440237

JP-SMF	Fluxnet 2015	2002-2006	30	MF	35.262	137.079	https://doi.org/10.18140/FLX/1440239
MY-PSO	Fluxnet 2015	2003-2009	77	EBF	2.973	102.306	https://doi.org/10.18140/FLX/1440240
NL-Hor	Fluxnet 2015	2004-2011	28	GRA	52.24	5.071	https://doi.org/10.18140/FLX/1440177
NL-Loo	Fluxnet 2015	1996-2014	121	ENF	52.167	5.744	https://doi.org/10.18140/FLX/1440178
PA-SPn	Fluxnet 2015	2007-2009	28	DBF	9.318	-79.635	https://doi.org/10.18140/FLX/1440180
PA-SPs	Fluxnet 2015	2007-2009	28	GRA	9.314	-79.631	https://doi.org/10.18140/FLX/1440179
RU-Cok	Fluxnet 2015	2003-2014	24	OSH	70.829	147.494	https://doi.org/10.18140/FLX/1440182
RU-Fyo	Fluxnet 2015	1998-2014	84	ENF	56.462	32.922	https://doi.org/10.18140/FLX/1440183
US-Blo	Fluxnet 2015	1997-2007	73	ENF	38.895	-120.633	https://doi.org/10.18140/FLX/1440068
US-Goo	Fluxnet 2015	2002-2006	27	GRA	34.255	-89.874	https://doi.org/10.18140/FLX/1440070
US-IB2	Fluxnet 2015	2004-2011	27	GRA	41.841	-88.241	https://doi.org/10.18140/FLX/1440072
US-KS2	Fluxnet 2015	2003-2006	47	CSH	28.609	-80.672	https://doi.org/10.18140/FLX/1440075
US-Me3	Fluxnet 2015	2004-2009	40	ENF	44.315	-121.608	https://doi.org/10.18140/FLX/1440080
US-Oho	Fluxnet 2015	2004-2013	44	DBF	41.555	-83.844	https://doi.org/10.18140/FLX/1440088
US-SRC	Fluxnet 2015	2008-2014	23	MF	31.908	-110.84	https://doi.org/10.18140/FLX/1440098
US-SRM	Fluxnet 2015	2004-2014	35	WSA	31.821	-110.866	https://doi.org/10.18140/FLX/1440090
US-UMB	Fluxnet 2015	2000-2014	63	DBF	45.56	-84.714	https://doi.org/10.18140/FLX/1440093
US-Wi4	Fluxnet 2015	2002-2005	21	ENF	46.739	-91.166	https://doi.org/10.18140/FLX/1440058

5 Non-Parametric Curve Fits

To fit curves to data points for visualization, we use a monotone copula smoother which projects all data points onto the 1:1 quantile line.

This is accomplished by (1) determining each data point's empirical marginal quantiles in each dimension, (2) averaging the marginal quantiles between the two dimensions and re-assigning both dimensions to this rank-averaged value, and (3) translating the re-assigned quantiles back into the original space using the original marginal quantile distribution for interpolation, treating the interpolation as independent for each variable. This compresses the points into an empirical bivariate curve (set of transformed points) with harmonized quantiles so that each point has the same rank in both dimensions. This is in some sense a best reduction in quantile-sorting errors given an underlying functional monotonicity assumption. The method is symmetric with respect to the two variables, and does not assume a direction or form of error structure (Short Gianotti, 2025).

The direction of monotonicity used is determined by the covariance of the data. For positive off-diagonal entries in the covariance matrix we use an increasing montonicity constraint, and for negative off-diagonal entries we use a decreasing monotonicity constraint.

While this method reduces variance, it maintains the same number of points, which can lead to fine-scale stair-stepping behavior. For simpler visualization, and to not suggest undue precision, we sub-sample these curves in Main Text Figures 1 and 2 to show on the order of 15 evenly-spaced (in a rank-sense) co-ordinates. In the Supplemental Material the curves are shown without sub-sampling (Supplemental Figure 1).

The fit curves are not used in any quantitative analyses, and are solely for visualization purposes.

6 Monthly Temporal Dynamics by Site and IGBP Class

Figure S2 shows the GPP-EF relationships monthly at all sites analyzed in the study, as in Main Text Figure 1. Each distinct line is a non-parametric curve-fit with no sub-sampling, fit using the method of Short Gianotti (2025). Due to the lack of sub-sampling, the curves appear less smooth than the curves in Main Text Figure 1, as they follow every monthly observation. Monotonicity is determined by sign of the covariance of all data for the site. Note the variability both within and across IGBP classes.

7 Dynamical Systems Estimation

We use regression-based dynamical systems models to show trajectories within phase spaces (Main Text Figures 2d, 3a,d,g). For each 2D dynamical system, we fit a system of first-order autonomous differential equations of the following form:

$$\begin{aligned} \frac{\mathrm{d}X}{\mathrm{d}t} &= a_1 + a_2 X + a_3 Y + a_4 X^2 + a_5 Y^2 + a_6 XY \\ \frac{\mathrm{d}Y}{\mathrm{d}t} &= b_1 + b_2 X + b_3 Y + b_4 X^2 + b_5 Y^2 + b_6 XY \end{aligned} \tag{Main Text 6}$$

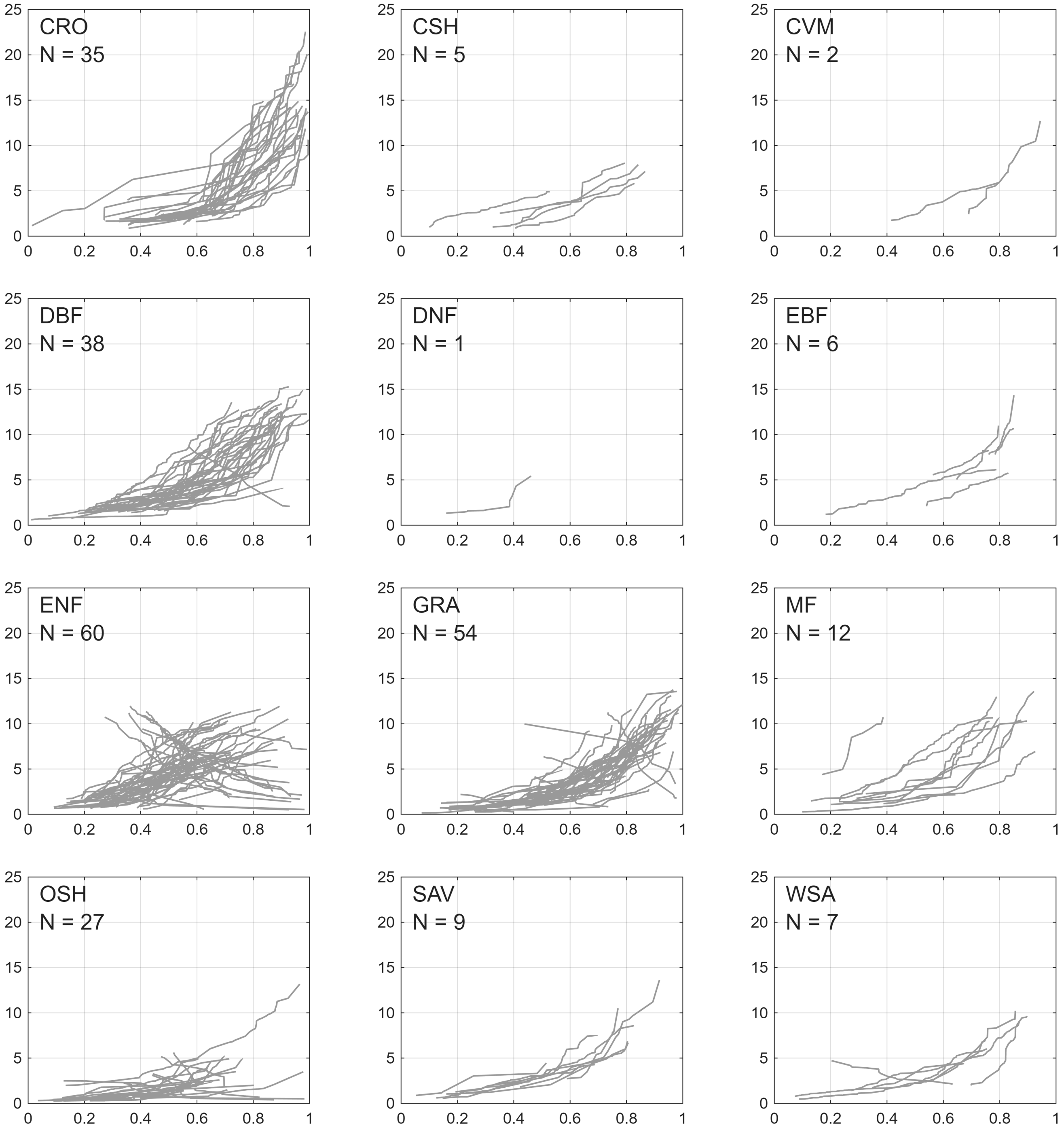
CRO
N = 35
CSH
N = 5
CVM
N = 2
DBF
N = 38
DNF
N = 1
EBF
N = 6
ENF
N = 60
GRA
N = 54
MF
N = 12
OSH
N = 27
SAV
N = 9
WSA
N = 7

Fig. S2. Monthly temporal dynamics at all sites, separated by IGBP class. Each curve shows a non-parametric curve fit to all growing season monthly values of GPP and EF for a single site, as in Main Text Figure 1. Each panel shows all sites analyzed within a given IGBP class, and N is the number of sites in that class. IGBP abbreviations are as follows: CRO: Cropland, CSH: Closed Shrubland, CVM: Cropland/Natural Vegetation Mosaic, DBF: Deciduous Broadleaf Forest, DNF: Deciduous Needleleaf Forest, EBF: Evergreen Broadleaf Forest, ENF: Evergreen Needleleaf Forest, GRA: Grassland, MF: Mixed Forest, OSH: Open Shrubland, SAV: Savanna, WSA: Woody Savanna.

This is a generic 1st-order nonlinear (quadratic) time-invariant dynamical system, i.e., the most basic, empirical representation of system dynamics allowing for quadratic non-linearity. This form is motivated by previous work which fit linear 1st-order dynamical systems at individual locations, which displayed non-linear attractor dynamics across space (Short Gianotti et al., 2024). This form allows for implicit differences across biogeography (through different states within the phase space), but with an implicit assumption that all spatial locations follow the same underlying functional dynamics with reference to the primary state variables.

The dynamical systems are fit to all data within the first 25 days of drydowns (using days beyond 25 has little impact on results—not shown—due to very low signal-to-noise ratios). To fit the system, we bin the phase space into an evenly-divided 50×50 grid. In each grid box, we collect all daily observations in the matching X and Y ranges, and calculate the first temporal differences for each observation in its corresponding drydown. The X, Y, $\mathrm{d}X/\mathrm{d}t$, and $\mathrm{d}Y/\mathrm{d}t$ values form a 4-value vector for each observation, and all observations for all growing season days across all sites are used to estimate the 12 parameters of Equation 6. The $\mathrm{d}X/\mathrm{d}t$, and $\mathrm{d}Y/\mathrm{d}t$ values are paired with the first of the two days' X and Y values.

The estimated system defines a flow field and trajectories through the phase space (Main Text Figures 2d, 3adg). Precipitation events shock the system to a new state in the state space, and the typical response for any site is to follow the flow lines from there.

Representations of the mean relationships between GPP–EF, f_v–EF, and $\omega_c\phi$–EF are shown in Main Figure 3. These are calculated using all daily values of the variables, including wet days, and calculating the mean values binned by the daily EF values. Uncertainties in the mean lines are calculated by bootstrapping all of the daily data with replacement 5,000 times. The standard error of the mean is shown in gray shading for each relationship. The curves and uncertainties are the same within each column.

Daily-scale regressions are calculated to quantify the simple, linear, bivariate relationships immediately after rain (Main Text Figure 3beh). To calculate the site-wise daily slopes between GPP and EF in Figure 3b, we take all points (EF($t = 1$), GPP($t = 1$)) the day immediately after rain at that site and connect them to points (EF($t = 2$), GPP($t = 2$)) the following day. This leads to one line segment for each drydown connecting the first two days in the GPP–EF space. For each site, We summarize these relationships across all drydowns using the median slope and median intercept of all segments for the site. Each site's median line is plotted, and the range shown depicts where the line passes through the box from the 25th quantile of EF($t = 1$) values (left), the 25th quantile of GPP($t = 1$) values (bottom), the 75th quantile of EF($t = 2$) values (right), and the 75th quantile of GPP($t = 2$) values (top). This roughly coincides with the central 50% of the data range for days 1 and 2 of drydowns for that site. The slopes of the lines shown are also displayed as a distribution in the inset figure (blue pdf, distributions of slopes across all sites). The same method is applied to the f_v–EF and $\omega_c\phi$–EF relationships (Main Text Figure 3eh).

To assess the changing relationships on multi-day timescales, we perform the same analysis using the first 4 days of each drydown. To calculate the linear representations of each drydown we use the Sen slope (median of all line segments) and median intercept. Following this, we again take the median slope for all of these drydown-specific lines to get a single characteristic slope for the first 4 days of drydowns for each site. These site-based slopes are shown in the green pdf in the inset figures of Main Text Figure 3beh. The same follows for 7-day and 10-day drydown periods (orange and red, respectively in the insets). This analysis is carried out for each of the GPP–EF, f_v–EF, and $\omega_c\phi$–EF relationships.

8 Role of ET

In Main Text Equation 3, GPP_l is the product of four terms, f_v, ω_c, ET_l, and ϕ. In the analyses of the manuscript, we group ω_c and ϕ together as our intensive variables and use f_v as our extensive analysis variable. Here we provide equivalent analysis of the remaining intensive variable, ET_l.

We use EF as our water-coupling variable in this study for two reasons. (1) Because EF is a water flux normalized by available energy, it controls for biogeographic differences in the local surface energy balance–for example incoming solar radiation and temperature effects as functions of latitudinal differences. (2) Relatedly, the empirical relationship between GPP and EF is somewhat stronger across sites than the GPP – ET or GPP – LE relationship (Short Gianotti et al., 2024), despite GPP and f_v also being correlated with the surface energy balance. Because of this, the GPP – EF relationship is the more applicable benchmark for comparing models with observations (e.g., Short Gianotti et al., 2024).

Figure S3 shows the dynamics for ET and EF, as a similar constituent component of GPP_l in Main Text Figure 3. In the main manuscript, we conclude that the long-term mean relationship between GPP and f_v in water-carbon coupling, as seen in their joint density and mean curve, is far stronger than the corresponding GPP_l-$\omega_c\phi$ relationship. This is apparent because both GPP_l and f_v co-vary with our water-cycle variable EF in qualitatively similar ways—both with positive, convex slopes. The ET – EF relationship dynamics shown in Figure S3 show a positive relationship in the mean and in typical system evolution. The relationship is not convex, but instead is nearly linear except for at the highest EF values, where curvature becomes negative. The relationship is largely expected, since EF is an energy-normalized version of ET.

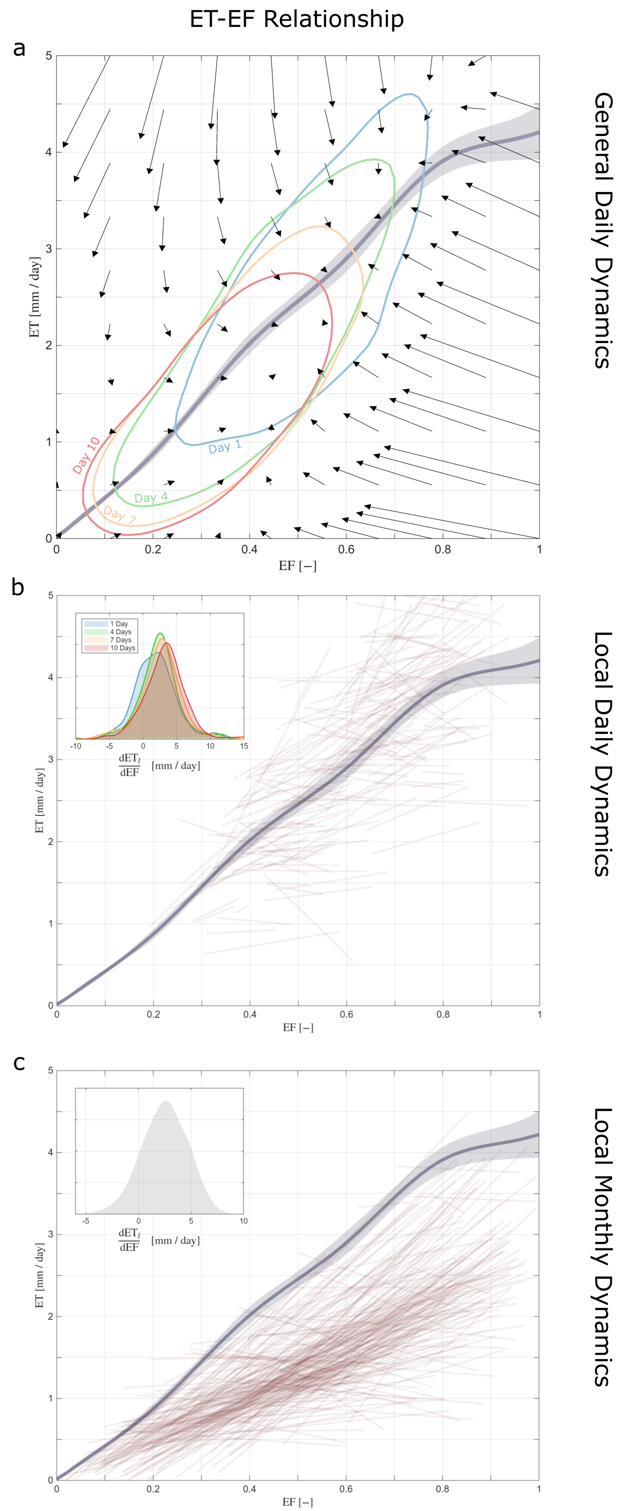

ET-EF Relationship
a
General Daily Dynamics
ET [mm / day]
EF [−]
Day 1
Day 4
Day 7
Day 10
b
Local Daily Dynamics
1 Day
4 Days
7 Days
10 Days
ET [mm / day]
EF [−]
c
Local Monthly Dynamics
ET [mm / day]
EF [−]

Fig. S3. Relationship between ET and EF dynamics. Evapotranspiration (ET) dynamics with evaporative fraction (EF), as in Main Text Figure 3. (a) Daily ET – EF dynamics for all flux towers after rainfall. Colored curves contain 50% of observations for the 1st, 4th, 7th, and 10th days after rainfall and move towards the origin (desiccated). Curve and shading show the empirical mean daily growing-season ET – EF relationship with bootstrapped standard error, including rain days. (b) ET – EF regressions for the first day after rain (day 2 minus day 1); each red line is a fit for a single tower site. Inset histogram shows the across-sites distribution of dET/dEF slopes for the first 1, 4, 7, and 10 days post rain. Curve and shading as in (a). (c) Linear regression fits for monthly-averaged ET – EF values within the growing season, depicting slower sub-seasonal dynamics. Histogram shows across-site distribution of regression slopes. Curve and shading as in (a).

9 Eddy Covariance Tower Citations

[CA-Ca1] T. Andrew Black (2018), AmeriFlux BASE CA-Ca1 British Columbia - 1949 Douglas-fir stand, Ver. 1-5, AmeriFlux AMP, (Dataset).
https://doi.org/10.17190/AMF/1480300

[CA-Ca2] T. Andrew Black (2018), AmeriFlux BASE CA-Ca2 British Columbia - Clearcut Douglas-fir stand (harvested winter 1999/2000), Ver. 1-5, AmeriFlux AMP, (Dataset).
https://doi.org/10.17190/AMF/1480301

[CA-Ca3] T. Andrew Black (2023), AmeriFlux BASE CA-Ca3 British Columbia - Pole sapling Douglas-fir stand, Ver. 5-5, AmeriFlux AMP, (Dataset).
https://doi.org/10.17190/AMF/1480302

[CA-LP1] Thomas Andrew Black (2021), AmeriFlux BASE CA-LP1 British Columbia - Mountain pine beetle-attacked lodgepole pine stand , Ver. 2-5, AmeriFlux AMP, (Dataset).
https://doi.org/10.17190/AMF/1660337

[CA-TP1] M. Altaf Arain (2018), AmeriFlux BASE CA-TP1 Ontario - Turkey Point 2002 Plantation White Pine, Ver. 3-5, AmeriFlux AMP, (Dataset).
https://doi.org/10.17190/AMF/1246009

[CA-TP4] M. Altaf Arain (2018), AmeriFlux BASE CA-TP4 Ontario - Turkey Point 1939 Plantation White Pine, Ver. 4-5, AmeriFlux AMP, (Dataset).
https://doi.org/10.17190/AMF/1246012

[US-Bi1] Camilo Rey-Sanchez, Carlos Tianxin Wang, Daphne Szutu, Robert Shortt, Samuel D. Chamberlain, Joseph Verfaillie, Dennis Baldocchi (2022), AmeriFlux BASE US-Bi1 Bouldin Island Alfalfa, Ver. 8-5, AmeriFlux AMP, (Dataset).
https://doi.org/10.17190/AMF/1480317

[US-CMW] Russell Scott (2022), AmeriFlux BASE US-CMW Charleston Mesquite Woodland, Ver. 2-5, AmeriFlux AMP, (Dataset).
https://doi.org/10.17190/AMF/1660339

[US-EML] Rosvel Bracho, Gerardo Celis, Heidi Rodenhizer, Craig See, Edward A. Schuur (2021), AmeriFlux BASE US-EML Eight Mile Lake Permafrost thaw gradient, Healy Alaska., Ver. 4-5, AmeriFlux AMP, (Dataset).
https://doi.org/10.17190/AMF/1418678

[US-ICh] Eugenie Euskirchen, Gaius Shaver, Syndonia Bret-Harte (2022), AmeriFlux BASE US-ICh Imnavait Creek Watershed Heath Tundra, Ver. 4-5, AmeriFlux AMP, (Dataset).
https://doi.org/10.17190/AMF/1246133

[US-Kon] Nathaniel Brunsell (2020), AmeriFlux BASE US-Kon Konza Prairie LTER (KNZ), Ver. 5-5, AmeriFlux AMP, (Dataset).
https://doi.org/10.17190/AMF/1246068

[US-LL1] Gregory Starr (2021), AmeriFlux BASE US-LL1 Longleaf Pine - Baker (Mesic site), Ver. 1-5, AmeriFlux AMP, (Dataset).
https://doi.org/10.17190/AMF/1773395

[US-LL2] Gregory Starr (2021), AmeriFlux BASE US-LL2 Longleaf Pine - Dubignion (Intermediate site), Ver. 1-5, AmeriFlux AMP, (Dataset).
https://doi.org/10.17190/AMF/1773396

[US-LL3] Gregory Starr (2021), AmeriFlux BASE US-LL3 Longleaf Pine - Red Dirt (Xeric site), Ver. 1-5, AmeriFlux AMP, (Dataset).
https://doi.org/10.17190/AMF/1773397

[US-LS1] Russell Scott (2020), AmeriFlux BASE US-LS1 San Pedro River Lewis Springs Sacaton Grassland, Ver. 1-5, AmeriFlux AMP, (Dataset).
https://doi.org/10.17190/AMF/1660346

[US-LS2] Russell Scott (2020), AmeriFlux BASE US-LS2 San Pedro River Lewis Springs Savanna, Ver. 1-5, AmeriFlux AMP, (Dataset).
https://doi.org/10.17190/AMF/1660347

[US-Me2] Bev Law (2022), AmeriFlux BASE US-Me2 Metolius mature ponderosa pine, Ver. 18-5, AmeriFlux AMP, (Dataset).
https://doi.org/10.17190/AMF/1246076

[US-Ne2] Andy Suyker (2022), AmeriFlux BASE US-Ne2 Mead - irrigated maize-soybean rotation site, Ver. 12-5, AmeriFlux AMP, (Dataset).
https://doi.org/10.17190/AMF/1246085

[US-Ne3] Andy Suyker (2022), AmeriFlux BASE US-Ne3 Mead - rainfed maize-soybean rotation site, Ver. 12-5, AmeriFlux AMP, (Dataset).
https://doi.org/10.17190/AMF/1246086

[US-PFa] Ankur Desai (2023), AmeriFlux BASE US-PFa Park Falls/WLEF, Ver. 24-5, AmeriFlux AMP, (Dataset).
https://doi.org/10.17190/AMF/1246090

[US-Prr] Go Iwahana, Hideki Kobayashi, Hiroki Ikawa, Rikie Suzuki (2019), AmeriFlux BASE US-Prr Poker Flat Research Range Black Spruce Forest, Ver. 3-5, AmeriFlux AMP, (Dataset).
https://doi.org/10.17190/AMF/1246153

[US-Rpf] Masahito Ueyama, Hiroki Iwata, Yoshinobu Harazono (2021), AmeriFlux BASE US-Rpf Poker Flat Research Range: Succession from fire scar to deciduous forest, Ver. 6-5, AmeriFlux AMP, (Dataset).
https://doi.org/10.17190/AMF/1579540

[US-Syv] Ankur Desai (2023), AmeriFlux BASE US-Syv Sylvania Wilderness Area, Ver. 23-5, AmeriFlux AMP, (Dataset).
https://doi.org/10.17190/AMF/1246106

[US-Ton] Siyan Ma, Liukang Xu, Joseph Verfaillie, Dennis Baldocchi (2022), AmeriFlux BASE US-Ton Tonzi Ranch, Ver. 16-5, AmeriFlux AMP, (Dataset).
https://doi.org/10.17190/AMF/1245971

[US-Uaf] Masahito Ueyama, Hiroki Iwata, Yoshinobu Harazono (2023), AmeriFlux BASE US-Uaf University of Alaska, Fairbanks, Ver. 11-5, AmeriFlux AMP, (Dataset).
https://doi.org/10.17190/AMF/1480322

[US-Var] Siyan Ma, Liukang Xu, Joseph Verfaillie, Dennis Baldocchi (2022), AmeriFlux BASE US-Var Vaira Ranch- Ione, Ver. 18-5, AmeriFlux AMP, (Dataset).
https://doi.org/10.17190/AMF/1245984

[US-WCr] Ankur Desai (2022), AmeriFlux BASE US-WCr Willow Creek, Ver. 24-5, AmeriFlux AMP, (Dataset).
https://doi.org/10.17190/AMF/1246111

[BR-Npw] George Vourlitis, Higo Dalmagro, José de S. Nogueira, Mark Johnson, Paulo Arruda (2019), AmeriFlux BASE BR-Npw Northern Pantanal Wetland, Ver. 1-5, AmeriFlux AMP, (Dataset).
https://doi.org/10.17190/AMF/1579716

[CA-Cbo] Ralf Staebler (2022), AmeriFlux BASE CA-Cbo Ontario - Mixed Deciduous, Borden Forest Site, Ver. 6-5, AmeriFlux AMP, (Dataset).
https://doi.org/10.17190/AMF/1498755

[CA-TP3] M. Altaf Arain (2018), AmeriFlux BASE CA-TP3 Ontario - Turkey Point 1974 Plantation White Pine, Ver. 3-5, AmeriFlux AMP, (Dataset).
https://doi.org/10.17190/AMF/1246011

[CA-TPD] M. Altaf Arain (2018), AmeriFlux BASE CA-TPD Ontario - Turkey Point Mature Deciduous, Ver. 2-5, AmeriFlux AMP, (Dataset).
https://doi.org/10.17190/AMF/1246152

[US-ARM] Sebastien Biraud, Marc Fischer, Stephen Chan, Margaret Torn (2023), AmeriFlux BASE US-ARM ARM Southern Great Plains site- Lamont, Ver. 12-5, AmeriFlux AMP, (Dataset).
https://doi.org/10.17190/AMF/1246027

[US-BZS] Eugenie Euskirchen (2022), AmeriFlux BASE US-BZS Bonanza Creek Black Spruce, Ver. 3-5, AmeriFlux AMP, (Dataset).
https://doi.org/10.17190/AMF/1756434

[US-GLE] John Frank, Bill Massman (2021), AmeriFlux BASE US-GLE GLEES, Ver. 8-5, AmeriFlux AMP, (Dataset).
https://doi.org/10.17190/AMF/1246056

[US-Ha1] J. William Munger (2022), AmeriFlux BASE US-Ha1 Harvard Forest EMS Tower (HFR1), Ver. 19-5, AmeriFlux AMP, (Dataset).
https://doi.org/10.17190/AMF/1246059

[US-Ho2] David Hollinger (2021), AmeriFlux BASE US-Ho2 Howland Forest (west tower), Ver. 4-5, AmeriFlux AMP, (Dataset).
https://doi.org/10.17190/AMF/1246062

[US-Jo1] Craig Tweedie (2023), AmeriFlux BASE US-Jo1 Jornada Experimental Range Bajada Site, Ver. 3-5, AmeriFlux AMP, (Dataset).
https://doi.org/10.17190/AMF/1767833

[US-Jo2] Enrique R. Vivoni, Eli R. Perez-Ruiz (2022), AmeriFlux BASE US-Jo2 Jornada Experimental Range Mixed Shrubland, Ver. 2-5, AmeriFlux AMP, (Dataset).
https://doi.org/10.17190/AMF/1617696

[US-KFS] Nathaniel Brunsell (2020), AmeriFlux BASE US-KFS Kansas Field Station, Ver. 7-5, AmeriFlux AMP, (Dataset). https://doi.org/10.17190/AMF/1246132

[US-KLS] Nathaniel Brunsell (2021), AmeriFlux BASE US-KLS Kansas Land Institute, Ver. 2-5, AmeriFlux AMP, (Dataset). https://doi.org/10.17190/AMF/1498745

[US-MMS] Kim Novick, Rich Phillips (2023), AmeriFlux BASE US-MMS Morgan Monroe State Forest, Ver. 22-5, AmeriFlux AMP, (Dataset).
https://doi.org/10.17190/AMF/1246080

[US-MOz] Jeffrey Wood, Lianhong Gu (2022), AmeriFlux BASE US-MOz Missouri Ozark Site, Ver. 11-5, AmeriFlux AMP, (Dataset).
https://doi.org/10.17190/AMF/1246081

[US-Mpj] Marcy Litvak (2022), AmeriFlux BASE US-Mpj Mountainair Pinyon-Juniper Woodland, Ver. 20-5, AmeriFlux AMP, (Dataset).
https://doi.org/10.17190/AMF/1246123

[US-NC1] Asko Noormets (2018), AmeriFlux BASE US-NC1 NC_Clearcut, Ver. 3-5, AmeriFlux AMP, (Dataset). https://doi.org/10.17190/AMF/1246082

[US-NR1] Peter D. Blanken, Russel K. Monson, Sean P. Burns, David R. Bowling, Andrew A. Turnipseed (2022), AmeriFlux BASE US-NR1 Niwot Ridge Forest (LTER NWT1), Ver. 19-5, AmeriFlux AMP, (Dataset).
https://doi.org/10.17190/AMF/1246088

[US-Ne1] Andy Suyker (2023), AmeriFlux BASE US-Ne1 Mead - irrigated continuous maize site, Ver. 14-5, AmeriFlux AMP, (Dataset).
https://doi.org/10.17190/AMF/1246084

[US-ONA] Maria Silveira (2022), AmeriFlux BASE US-ONA Florida pine flatwoods, Ver. 3-5, AmeriFlux AMP, (Dataset). https://doi.org/10.17190/AMF/1660350

[US-Rms] Gerald Flerchinger (2021), AmeriFlux BASE US-Rms RCEW Mountain Big Sagebrush, Ver. 4-5, AmeriFlux AMP, (Dataset).
https://doi.org/10.17190/AMF/1375202

[US-Ro1] John Baker, Tim Griffis, Timothy Griffis (2018), AmeriFlux BASE US-Ro1 Rosemount- G21, Ver. 5-5, AmeriFlux AMP, (Dataset).
https://doi.org/10.17190/AMF/1246092

[US-Rwe] Gerald Flerchinger, Michele L. Reba (2020), AmeriFlux BASE US-Rwe RCEW Reynolds Mountain East, Ver. 1-5, AmeriFlux AMP, (Dataset).
https://doi.org/10.17190/AMF/1617721

[US-Rwf] Gerald Flerchinger (2021), AmeriFlux BASE US-Rwf RCEW Upper Sheep Prescibed Fire, Ver. 2-5, AmeriFlux AMP, (Dataset).
https://doi.org/10.17190/AMF/1617724

[US-Rws] Gerald Flerchinger (2021), AmeriFlux BASE US-Rws Reynolds Creek Wyoming big sagebrush, Ver. 4-5, AmeriFlux AMP, (Dataset).
https://doi.org/10.17190/AMF/1375201

[US-Seg] Marcy Litvak (2022), AmeriFlux BASE US-Seg Sevilleta grassland, Ver. 20-5, AmeriFlux AMP, (Dataset).
https://doi.org/10.17190/AMF/1246124

[US-Ses] Marcy Litvak (2022), AmeriFlux BASE US-Ses Sevilleta shrubland, Ver. 20-5, AmeriFlux AMP, (Dataset).
https://doi.org/10.17190/AMF/1246125

[US-Sne] Robert Shortt, Kyle Hemes, Daphne Szutu, Joseph Verfaillie, Dennis Baldocchi (2021), AmeriFlux BASE US-Sne Sherman Island Restored Wetland, Ver. 7-5, AmeriFlux AMP, (Dataset).
https://doi.org/10.17190/AMF/1418684

[US-Tw3] Samuel D Chamberlain, Patty Oikawa, Cove Sturtevant, Daphne Szutu, Joseph Verfaillie, Dennis Baldocchi (2018), AmeriFlux BASE US-Tw3 Twitchell Alfalfa, Ver. 5-5, AmeriFlux AMP, (Dataset).
https://doi.org/10.17190/AMF/1246149

[US-UMd] Christopher Gough, Gil Bohrer, Peter Curtis (2022), AmeriFlux BASE US-UMd UMBS Disturbance, Ver. 12-5, AmeriFlux AMP, (Dataset).
https://doi.org/10.17190/AMF/1246134

[US-Whs] Russ Scott (2023), AmeriFlux BASE US-Whs Walnut Gulch Lucky Hills Shrub, Ver. 20-5, AmeriFlux AMP, (Dataset).
https://doi.org/10.17190/AMF/1246113

[US-Wjs] Marcy Litvak (2022), AmeriFlux BASE US-Wjs Willard Juniper Savannah, Ver. 19-5, AmeriFlux AMP, (Dataset).
https://doi.org/10.17190/AMF/1246120

[US-Wkg] Russell Scott (2023), AmeriFlux BASE US-Wkg Walnut Gulch Kendall Grasslands, Ver. 20-5, AmeriFlux AMP, (Dataset).
https://doi.org/10.17190/AMF/1246112

[US-xBR] NEON (National Ecological Observatory Network) (2022), AmeriFlux BASE US-xBR NEON Bartlett Experimental Forest (BART), Ver. 6-5, AmeriFlux AMP, (Dataset).
https://doi.org/10.17190/AMF/1579542

[US-xDS] NEON (National Ecological Observatory Network) (2022), AmeriFlux BASE US-xDS NEON Disney Wilderness Preserve (DSNY), Ver. 5-5, AmeriFlux AMP, (Dataset).
https://doi.org/10.17190/AMF/1671895

[US-xHA] NEON (National Ecological Observatory Network) (2022), AmeriFlux BASE US-xHA NEON Harvard Forest (HARV), Ver. 7-5, AmeriFlux AMP, (Dataset).
https://doi.org/10.17190/AMF/1562391

[US-xJE] NEON (National Ecological Observatory Network) (2022), AmeriFlux BASE US-xJE NEON Jones Ecological Research Center (JERC), Ver. 6-5, AmeriFlux AMP, (Dataset).
https://doi.org/10.17190/AMF/1617730

[US-xSB] NEON (National Ecological Observatory Network) (2022), AmeriFlux BASE US-xSB NEON Ordway-Swisher Biological Station (OSBS), Ver. 5-5, AmeriFlux AMP, (Dataset).
https://doi.org/10.17190/AMF/1671899

[US-xTA] NEON (National Ecological Observatory Network) (2022), AmeriFlux BASE US-xTA NEON Talladega National Forest (TALL), Ver. 5-5, AmeriFlux AMP, (Dataset).
https://doi.org/10.17190/AMF/1671902

[US-xTR] NEON (National Ecological Observatory Network) (2022), AmeriFlux BASE US-xTR NEON Treehaven (TREE), Ver. 6-5, AmeriFlux AMP, (Dataset).
https://doi.org/10.17190/AMF/1634886

[US-xUN] NEON (National Ecological Observatory Network) (2022), AmeriFlux BASE US-xUN NEON University of Notre Dame Environmental Research Center (UNDE), Ver. 6-5, AmeriFlux AMP, (Dataset).
https://doi.org/10.17190/AMF/1617741

[AT-Neu] Wohlfahrt, G., Hammerle, A., Haslwanter, A., Bahn, M., Tappeiner, U. and Cernusca, A.: Seasonal and inter-annual variability of the net ecosystem CO2 exchange of a temperate mountain grassland: Effects of weather and management, J. Geophys. Res., 113(D8), D08110, 2008.

[AU-Cpr] Meyer, W. S., Kondrlovà, E. and Koerber, G. R.: Evaporation of perennial semi-arid woodland in southeastern Australia is adapted for irregular but common dry periods, Hydrol. Process., 29(17), 3714–3726, 2015.

[AU-Cum] Beringer, J., Hutley, L. B., McHugh, I., Arndt, S. K., Campbell, D., Cleugh, H. A., ... & Wardlaw, T. (2016). An introduction to the Australian and New Zealand flux tower network–OzFlux. Biogeosciences, 13(21), 5895-5916.

[AU-DaP] Beringer, J., Hutley, L. B., Hacker, J. M., Neininger, B. and Paw U, K. T.: Patterns and processes of carbon, water and energy cycles across northern Australian landscapes: From point to region, Agric. For. Meteorol., 151(11), 1409–1416, 2011a.

[AU-DaS] Hutley, L. B., Beringer, J., Isaac, P. R., Hacker, J. M. and Cernusak, L. A.: A sub-continental scale living laboratory: Spatial patterns of savanna vegetation over a rainfall gradient in northern Australia, Agric. For. Meteorol., 151(11), 1417–1428, 2011.

[AU-Dry] Cernusak, L. A., Hutley, L. B., Beringer, J., Holtum, J. A. M. and Turner, B. L.: Photosynthetic physiology of eucalypts along a sub-continental rainfall gradient in northern Australia, Agric. For. Meteorol., 151(11), 1462–1470, 2011.

[AU-GWW] Craig Macfarlane, Suzanne Prober, Georg Wiehl (2013-2014) FLUXNET2015 AU-GWW Great Western Woodlands, Western Australia, Australia, Dataset.
https://doi.org/10.18140/FLX/1440200

[AU-Gin] Craig Macfarlane, Patricia Lambert, John Byrne, Chris Johnstone, Natalie Smart (2011-2014) FLUXNET2015 AU-Gin Gingin, Dataset.
https://doi.org/10.18140/FLX/1440199

[AU-How] Beringer, J., Hutley, L. B., Tapper, N. J. and Cernusak, L. A.: Savanna fires and their impact on net ecosystem productivity in North Australia, Glob. Chang. Biol., 13(5), 990–1004, 2007.

[AU-Rig] Beringer, J., Hutley, L. B., McHugh, I., Arndt, S. K., Campbell, D., Cleugh, H. A., ... & Wardlaw, T. (2016). An introduction to the Australian and New Zealand flux tower network–OzFlux. Biogeosciences, 13(21), 5895-5916.

[AU-Stp] Beringer, J., Hutley, L. B., Hacker, J. M., Neininger, B. and Paw U, K. T.: Patterns and processes of carbon, water and energy cycles across northern Australian landscapes: From point to region, Agric. For. Meteorol., 151(11), 1409–1416, 2011a.

[AU-Tum] Leuning, R., Cleugh, H. A., Zegelin, S. J. and Hughes, D.: Carbon and water fluxes over a temperate Eucalyptus forest and a tropical wet/dry savanna in Australia: measurements and comparison with MODIS remote sensing estimates, Agric. For. Meteorol., 129(3–4), 151–173, 2005.

[AU-Wac] Kilinc, M., Beringer, J., Hutley, L. B., Tapper, N. J. and McGuire, D. A.: Carbon and water exchange of the world's tallest angiosperm forest, Agric. For. Meteorol., 182–183, 215–224, 2013.

[AU-Whr] McHugh, I. D., Beringer, J., Cunningham, S. C., Baker, P. J., Cavagnaro, T. R., Mac Nally, R. and Thompson, R. M.: Interactions between nocturnal turbulent flux, storage and advection at an “ideal” eucalypt woodland site, Biogeoscience, 14, 3027-3050, 2017.

[AU-Wom] Stefan Arndt, Nina Hinko-Najera, Anne Griebel, Jason Beringer, Stephen Livesley (2010-2014) FLUXNET2015 AU-Wom Wombat, Dataset.
https://doi.org/10.18140/FLX/1440207

[BE-Bra] Carrara, A., Janssens, I. A., Curiel Yuste, J. and Ceulemans, R.: Seasonal changes in photosynthesis, respiration and NEE of a mixed temperate forest, Agric. For. Meteorol., 126(1–2), 15–31, 2004.

[BE-Lon] Moureaux, C., Debacq, A., Bodson, B., Heinesch, B. and Aubinet, M.: Annual net ecosystem carbon exchange by a sugar beet crop, Agric. For. Meteorol., 139(1–2), 25–39, 2006.

[BE-Vie] Aubinet, M., Chermanne, B., Vandenhaute, M., Longdoz, B., Yernaux, M. and Laitat, E.: Long term carbon dioxide exchange above a mixed forest in the Belgian Ardennes, Agric. For. Meteorol., 108(4), 293–315, 2001.

[BR-Sa1] Baker, T. R., Phillips, O. L., Malhi, Y., Almeida, S., Arroyo, L., Di Fiore, A., Erwin, T., Killeen, T. J., Laurance, S. G., Laurance, W. F., Lewis, S. L., Lloyd, J., Monteagudo, A., Neill, D. A., Patino, S., Pitman, N. C., M. Silva, J. N., Vasquez Martinez, R. (2004) Variation In Wood Density Determines Spatial Patterns Inamazonian Forest Biomass, Global Change Biology, 10(5), 545-562.

[BR-Sa3] Asner, G. P., Keller, M., Pereira, Jr, R., Zweede, J. C., Silva, J. N. (2004) Canopy Damage And Recovery After Selective Logging In Amazonia: Field And Satellite Studies, Ecological Applications, 14(sp4), 280-298.

[CA-Gro] Barr, A., Richardson, A., Hollinger, D., Papale, D., Arain, M., Black, T., Bohrer, G., Dragoni, D., Fischer, M., Gu, L., Law, B., Margolis, H., McCaughey, J., Munger, J., Oechel, W., Schaeffer, K. (2013) Use Of Change-Point Detection For Friction–Velocity Threshold Evaluation In Eddy-Covariance Studies, Agricultural And Forest Meteorology, 171-172(7), 31-45.

[CA-Man] Amiro, B., MacPherson, J. I., Desjardins, R. L. (1999) Boreas Flight Measurements Of Forest-Fire Effects On Carbon Dioxide And Energy Fluxes, Agricultural And Forest Meteorology, 96(4), 199-208.

[CA-NS2] Baldocchi, D., Penuelas, J. (2018) The Physics And Ecology Of Mining Carbon Dioxide From The Atmosphere By Ecosystems, Global Change Biology, 45(11), 9275–9287.

[CA-NS3] Baldocchi, D., Penuelas, J. (2018) The Physics And Ecology Of Mining Carbon Dioxide From The Atmosphere By Ecosystems, Global Change Biology, 14(7), 074023.

[CA-Oas] Barr, A. G., Black, T., Hogg, E., Kljun, N., Morgenstern, K., Nesic, Z. (2004) Inter-Annual Variability In The Leaf Area Index Of A Boreal Aspen-Hazelnut Forest In Relation To Net Ecosystem Production, Agricultural And Forest Meteorology, 126(3-4), 237-255.

[CA-Obs] Barr, A., Richardson, A., Hollinger, D., Papale, D., Arain, M., Black, T., Bohrer, G., Dragoni, D., Fischer, M., Gu, L., Law, B., Margolis, H., McCaughey, J., Munger, J., Oechel, W., Schaeffer, K. (2013) Use Of Change-Point Detection For Friction–Velocity Threshold Evaluation In Eddy-Covariance Studies, Agricultural And Forest Meteorology, 171-172(5), 31-45.

[CA-Qfo] Baldocchi, D., Penuelas, J. (2018) The Physics And Ecology Of Mining Carbon Dioxide From The Atmosphere By Ecosystems, Global Change Biology, 45(1), 9275–9287.

[CA-SF1] Amiro, B. (2009) Measuring Boreal Forest Evapotranspiration Using The Energy Balance Residual, Journal Of Hydrology, 366(1-4), 112-118.

[CA-SF2] Amiro, B. (2009) Measuring Boreal Forest Evapotranspiration Using The Energy Balance Residual, Journal Of Hydrology, 366(1-4), 112-118.

[CA-SF3] Amiro, B. (2009) Measuring Boreal Forest Evapotranspiration Using The Energy Balance Residual, Journal Of Hydrology, 366(1-4), 112-118

[CH-Cha] Merbold, L., Eugster, W., Stieger, J., Zahniser, M., Nelson, D. and Buchmann, N.: Greenhouse gas budget (CO2, CH4 and N2O) of intensively managed grassland following restoration, Glob. Chang. Biol., 20(6), 1913–1928, 2014.

[CH-Dav] Zielis, S., Etzold, S., Zweifel, R., Eugster, W., Haeni, M. and Buchmann, N.: NEP of a Swiss subalpine forest is significantly driven not only by current but also by previous year's weather, Biogeosciences, 11(6), 1627–1635, 2014.

[CH-Fru] Imer, D., Merbold, L., Eugster, W. and Buchmann, N.: Temporal and spatial variations of soil CO2, CH4 and N2O fluxes at three differently managed grasslands, Biogeosciences, 10(9), 5931–5945, 2013.

[CH-Lae] Etzold, S., Ruehr, N. K., Zweifel, R., Dobbertin, M., Zingg, A., Pluess, P., Häsler, R., Eugster, W. and Buchmann, N.: The Carbon Balance of Two Contrasting Mountain Forest Ecosystems in Switzerland: Similar Annual Trends, but Seasonal Differences, Ecosystems, 14(8), 1289–1309, 2011.

[CH-Oe1] Ammann, C., Spirig, C., Leifeld, J. and Neftel, A.: Assessment of the nitrogen and carbon budget of two managed temperate grassland fields, Agric. Ecosyst. Environ., 133(3–4), 150–162, 2009.

[CH-Oe2] Dietiker D, Buchmann N, Eugster W (2010) Testing the ability of the DNDC model to predict CO2 and water vapour fluxes of a Swiss cropland site. Agriculture, Ecosystems and Environment 139: 396–401.

[CN-Din] Gui-Rui Yu a,*, Xue-Fa Wen a, Xiao-Min Sun a, Bertrand D. Tanner b, Xuhui Lee c, Jia-Yi Chen Overview of ChinaFLUX and evaluation of ist eddy covariance measurement Agricultural and Forest Meteorology 137 (2006) 125–137.

[CN-Qia] Gui-Rui Yu a,*, Xue-Fa Wen a, Xiao-Min Sun a, Bertrand D. Tanner b, Xuhui Lee c, Jia-Yi Chen Overview of ChinaFLUX and evaluation of ist eddy covariance measurement. Agricultural and Forest Meteorology 137 (2006) 125–137.

[CZ-BK1] Acosta, M., Pavelka, M., Montagnani, L., Kutsch, W., Lindroth, A., Juszczak, R. and Janouš, D.: Soil surface CO2 efflux measurements in Norway spruce forests: Comparison between four different sites across Europe — from boreal to alpine forest, Geoderma, 192, 295–303, 2013.

[CZ-BK2] Ladislav Sigut, Katerina Havrankova, Georg Jocher, Marian Pavelka, Dalibor Janouš, Karel Stanik, Jan Trusina, Radek Czerny (2004-2012) FLUXNET2015 CZ-BK2 Bily Kriz grassland, Dataset.
https://doi.org/10.18140/FLX/1440144

[DE-Geb] Anthoni, P. M., Knohl, A., Rebmann, C., Freibauer, A., Mund, M., Ziegler, W., Kolle, O. and Schulze, E.-D.: Forest and agricultural land-use-dependent CO2 exchange in Thuringia, Germany, Glob. Chang. Biol., 10(12), 2005–2019, 2004.

[DE-Gri] Prescher, A.-K., Grünwald, T., Bernhofer, C: Land use regulates carbon budgets in eastern Germany: From NEE to NBP. Agric. For. Meteorol., 150, 1016-1025, 2010.

[DE-Hai] Knohl, A., Schulze, E.-D., Kolle, O. and Buchmann, N.: Large carbon uptake by an unmanaged 250-year-old deciduous forest in Central Germany, Agric. For. Meteorol., 118(3–4), 151–167, 2003.

[DE-Kli] Prescher, A.-K., Grünwald, T., Bernhofer, C: Land use regulates carbon budgets in eastern Germany: From NEE to NBP. Agric. For. Meteorol., 150, 1016-1025, 2010.

[DE-Lkb] Lindauer, M., Schmid, H. P., Grote, R., Mauder, M., Steinbrecher, R. and Wolpert, B.: Net ecosystem exchange over a non-cleared wind-throw-disturbed upland spruce forest—Measurements and simulations, Agric. For. Meteorol., 197, 219–234, 2014.

[DE-Lnf] Anthoni, P. M., Knohl, A., Rebmann, C., Freibauer, A., Mund, M., Ziegler, W., Kolle, O. and Schulze, E.-D.: Forest and agricultural land-use-dependent CO2 exchange in Thuringia, Germany, Glob. Chang. Biol., 10(12), 2005–2019, 2004.

[DE-Obe] Christian Bernhofer, Thomas Grünwald, Uta Moderow, Markus Hehn, Uwe Eichelmann, Heiko Prasse, Udo Postel (2008-2014) FLUXNET2015 DE-Obe Oberbärenburg, Dataset.
https://doi.org/10.18140/FLX/1440151

[DE-RuR] Borchard, N., Schirrmann, M., von Hebel, C., Schmidt, M., Baatz, R., Les Firbank, L., Vereecken, H., Herbst, M., 2015: Spatio-temporal drivers of soil and ecosystem carbon fluxes at field scale in an upland grassland in Germany. AGEE, 211, 84-93.

[DE-Tha] Grünwald, T. and Bernhofer, C.: A decade of carbon, water and energy flux measurements of an old spruce forest at the Anchor Station Tharandt, Tellus B Chem. Phys. Meteorol., 59(3), 387–396, 2007.

[DK-Sor] Pilegaard, K., Ibrom, A., Courtney, M. S., Hummelshøj, P. and Jensen, N. O.: Increasing net CO2 uptake by a Danish beech forest during the period from 1996 to 2009, Agric. For. Meteorol., 151(7), 934–946, 2011.

[ES-Amo] López-Ballesteros, A., Serrano-Ortiz, P., Kowalski, A.S., Sánchez-Cañete, E.P., Scott, R.L. and Domingo F.: Subterranean ventilation of allochthonous CO governs net CO exchange in a semiarid Mediterranean grassland, Agricultural and Forest Meteorology, 234, 115-126, 2017.

[ES-LJu] Serrano-Ortiz, P., Domingo, F., Cazorla, A., Were, A., Cuezva, S., Villagarcía, L., Alados-Arboledas, L. and Kowalski, A.S.: Interannual CO2 exchange of a sparse Mediterranean shrubland on a carbonaceous substrate, J. Geophys. Res., 114, G04015, 2009.

[FI-Hyy] Suni, T., Rinne, J., Reissell, A., Altimir, N., Keronen, P., Rannik, Ü., Maso, M. D., Kulmala, M. and Vesala, T.: Long-term measurements of surface fluxes above a Scots pine forest in Hyytiälä, southern Finland, 1996–2001, BOREAL ENVIRONEMNT RESEARCH, 8, 287–301, 2003.

[FI-Sod] Thum, T., Aalto, T., Laurila, T., Aurela, M., Kolari, P. and Hari, P.: Parametrization of two photosynthesis models at the canopy scale in a northern boreal Scots pine forest, Tellus B Chem. Phys. Meteorol., 59(5), 874–890, 2007.

[FR-Fon] Bazot, S., Barthes, L., Blanot, D. & Fresneau, C. Distribution of non-structural nitrogen and carbohydrate compounds in mature oak trees in a temperate forest at four key phenological stages. Trees-Structure and Function 27, 1023-1034.

[FR-Gri] Loubet B., Laville P., Lehuger S., Larmanou E., Fléchard C., Mascher N., Génermont S., Roche R., Ferrara R.M., Stella P., Personne E., Durand B., Decuq C., Flura D., Masson S., Fanucci O., Rampon J.N., Siemens J., Kindler R., Gabrielle B., Schrumpf M. and Cellier P.: Carbon, nitrogen and Greenhouse gases budgets over a four years crop rotation in northern France Plant and Soil, 343, 1/2, 109–137, 2011.

[FR-LBr] Berbigier, P., Bonnefond, J.-M. and Mellmann, P.: CO2 and water vapour fluxes for 2 years above Euroflux forest site, Agric. For. Meteorol., 108(3), 183–197, 2001.

[FR-Pue] Rambal, S., Joffre, R., Ourcival, J. M., Cavender-Bares, J. and Rocheteau, A.: The growth respiration component in eddy CO2 flux from a Quercus ilex mediterranean forest, Glob. Chang. Biol., 10(9), 1460–1469, 2004.

[GF-Guy] Bonal, D., Bosc, A., Ponton, S., Goret, J.-Y., Burban, B., Gross, P., Bonnefond, J.-M., Elbers, J., Longdoz, B., Epron, D., Guehl, J.-M. and Granier, A.: Impact of severe dry season on net ecosystem exchange in the Neotropical rainforest of French Guiana, Glob. Chang. Biol., 14(8), 1917–1933, 2008.

[GH-Ank] Chiti, T., Certini, G., Grieco, E. and Valentini, R.: The role of soil in storing carbon in tropical rainforests: the case of Ankasa Park, Ghana, Plant Soil, 331, 453-461, 2010.

[GL-ZaH] Lund, M., Falk, J. M., Friborg, T., Mbufong, H. N., Sigsgaard, C., Soegaard, H. and Tamstorf, M. P.: Trends in CO2 exchange in a high Arctic tundra heath, 2000–2010, J. Geophys. Res., 117(G2), G02001, 2012.

[IT-BCi] Vitale, L., Di Tommasi, P., D'Urso, G. and Magliulo, V.: The response of ecosystem carbon fluxes to LAI and environmental drivers in a maize crop grown in two contrasting seasons, Int. J. Biometeorol., 60(3), 411–420, 2016.

[IT-Col] Valentini, R., De Angelis, P., Matteucci, G., Monaco, R., Dore, S. and Mugnozza, G. E. S.: Seasonal net carbon dioxide exchange of a beech forest with the atmosphere, Glob. Chang. Biol., 2(3), 199–207, 1996.

[IT-Cpz] Garbulsky, M.F., Penuelas, J., Papale, D., Filella, I.: Remote estimation of carbon dioxide uptake by a Mediterranean forest. Global Change Biology, 14, 2860–2867, 2008.

[IT-Lav] Marcolla. B., Pitacco, A., Cescatti, A.: Canopy architecture and turbulence structure in a Coniferous forest. Boundary-Layer Meteorology, 108, 39–59, 2003.

[IT-MBo] Marcolla, B., Cescatti, A., Manca, G., Zorer, R., Cavagna, M., Fiora, A., Gianelle, D., Rodeghiero, M., Sottocornola, M. and Zampedri, R.: Climatic controls and ecosystem responses drive the inter-annual variability of the net ecosystem exchange of an alpine meadow, Agric. For. Meteorol., 151(9), 1233–1243, 2011.

[IT-Noe] Marras S., Pyles R.D, Sirca C., Paw U K.T., Snyder R.L., Duce P., Spano D. 2011. Evaluation of the Advanced Canopy-Atmosphere-Soil Algorithm (ACASA) model performance over Mediterranean maquis ecosystem. Agricultural and Forest Meteorology 151: 730-745.

[IT-Ren] Montagnani, L., Manca, G., Canepa, E., Georgieva, E., Acosta, M., Feigenwinter, C., Janous, D., Kerschbaumer, G., Lindroth, A., Minach, L., Minerbi, S., Mölder, M., Pavelka, M., Seufert, G., Zeri, M. and Ziegler, W.: A new mass conservation approach to the study of CO2 advection in an alpine forest, J. Geophys. Res., 114(D7), D07306, 2009.

[IT-Ro1] Rey, A., Pegoraro, E., Tedeschi, V., De Parri, I., Jarvis, P. G. and Valentini, R.: Annual variation in soil respiration and its components in a coppice oak forest in Central Italy, Glob. Chang. Biol., 8(9), 851–866, 2002.

[IT-Ro2] Tedeschi, V., Rey, A., Manca, G., Valentini, R., Jarvis, P. G. and Borghetti, M.: Soil respiration in a Mediterranean oak forest at different developmental stages after coppicing, Glob. Chang. Biol., 12(1), 110–121, 2006.

[IT-SRo] Chiesi, M., Maselli, F., Bindi, M., Fibbi, L., Cherubini, P., Arlotta, E., Tirone, G., Matteucci, G. and Seufert, G.: Modelling carbon budget of Mediterranean forests using ground and remote sensing measurements, Agric. For. Meteorol., 135(1–4), 22–34, 2005.

[IT-Tor] Galvagno, M., Wohlfahrt, G., Cremonese, E., Rossini, M., Colombo, R., Filippa, G., Julitta, T., Manca, G., Siniscalco, C., di Cella, U. M. and Migliavacca, M.: Phenology and carbon dioxide source/sink strength of a subalpine grassland in response to an exceptionally short snow season, Environ. Res. Lett., 8(2), 025008, 2013.

[JP-SMF] Matsumoto, K., Ohta, T., Nakai, T., Kuwada, T., Daikoku, K., Iida, S., Yabuki, H., Kononov, A. V., van der Molen, M. K., Kodama, Y., Maximov, T. C., Dolman, A. J. and Hattori, S.: Energy consumption and evapotranspiration at several boreal and temperate forests in the Far East, Agric. For. Meteorol., 148(12), 1978–1989, 2008.

[MY-PSO] Yoshiko Kosugi, Satoru Takanashi (2003-2009) FLUXNET2015 MY-PSO Pasoh Forest Reserve (PSO), Dataset. https://doi.org/10.18140/FLX/1440240

[NL-Hor] Jacobs, C. M. J., Jacobs, A. F. G., Bosveld, F. C., Hendriks, D. M. D., Hensen, A., Kroon, P. S., Moors, E. J., Nol, L., Schrier-Uijl, A. and Veenendaal, E. M.: Variability of annual CO2 exchange from Dutch grasslands, Biogeosciences, 4(5), 803–816, 2007.

[NL-Loo] Moors, E. J.: Water Use of Forests in The Netherlands, PhD-thesis, Vrije Universiteit Amsterdam., the Netherlands, 2012.

[PA-SPn] Wolf, S., Eugster, W., Potvin, C., Turner, B. L. and Buchmann, N.: Carbon sequestration potential of tropical pasture compared with afforestation in Panama. Global Change Biology, 17: 2763–2780, 2011.

[PA-SPs] Wolf, S., Eugster, W., Potvin, C., Turner, B. L. and Buchmann, N.: Carbon sequestration potential of tropical pasture compared with afforestation in Panama. Global Change Biology, 17: 2763–2780, 2011.

[RU-Cok] van der Molen, M. K. van der, Huissteden, J. van, Parmentier, F. J. W., Petrescu, A. M. R., Dolman, A. J., Maximov, T. C., Kononov, A. V., Karsanaev, S. V. and Suzdalov, D. A.: The growing season greenhouse gas balance of a continental tundra site in the Indigirka lowlands, NE Siberia, Biogeosciences, 4(6), 985–1003, 2007.

[RU-Fyo] Kurbatova, J., Li, C., Varlagin, A., Xiao, X. and Vygodskaya, N.: Modeling carbon dynamics in two adjacent spruce forests with different soil conditions in Russia, Biogeosciences, 5(4), 969–980, 2008.

[US-Blo] Baker, B., Guenther, A., Greenberg, J., Goldstein, A., Fall, R. (1999) Canopy Fluxes Of 2-Methyl-3-Buten-2-Ol Over A Ponderosa Pine Forest By Relaxed Eddy Accumulation: Field Data And Model Comparison, Journal Of Geophysical Research: Atmospheres, 104(D21), 26107-26114.

[US-Goo] Benjamin R. K. Runkle, James R. Rigbyb, Michele L. Rebac, Saseendran S. Anapallid, Joydeep Bhattacharjeee, Ken W. Kraussf, Lu Liangg, Martin A. Locke, Kimberly A. Novick, Ruixiu Suid, Kosana Suvočareva and Paul M. White (2017) Delta-Flux: An Eddy Covariance Network for a Climate-Smart Lower Mississippi Basin, Agricultural & Environmental Letters, 2(1).

[US-IB2] Allison, V. J., Miller, R. M., Jastrow, J. D., Matamala, R., Zak, D. R. (2005) Changes In Soil Microbial Community Structure In A Tallgrass Prairie Chronosequence, Soil Science Society Of America Journal, 69(5), 1412-1421.

[US-KS2] Baldocchi, D., Penuelas, J. (2018) The Physics And Ecology Of Mining Carbon Dioxide From The Atmosphere By Ecosystems, Global Change Biology, 207(1), 117-126.

[US-Me3] Barr, A., Richardson, A., Hollinger, D., Papale, D., Arain, M., Black, T., Bohrer, G., Dragoni, D., Fischer, M., Gu, L., Law, B., Margolis, H., McCaughey, J., Munger, J., Oechel, W., Schaeffer, K. (2013) Use Of Change-Point Detection For Friction–Velocity Threshold Evaluation In Eddy-Covariance Studies, Agricultural And Forest Meteorology, 171-172(1), 31-45.

[US-Oho] Chu, H., Baldocchi, D. D., Poindexter, C., Abraha, M., Desai, A. R., Bohrer, G., Arain, M. A., Griffis, T., Blanken, P. D., OHalloran, T. L., Thomas, R. Q., Zhang, Q., Burns, S. P., Frank, J. M., Christian, D., Brown, S., Black, T. A., Gough, C. M., Law, B. E., Lee, X., Chen, J., Reed, D. E., Massman, W. J., Clark, K., Hatfield, J., Prueger, J., Bracho, R., Baker, J. M., Martin, T. A. (2018) Temporal Dynamics Of Aerodynamic Canopy Height Derived From Eddy Covariance Momentum Flux Data Across North American Flux Networks, Geophysical Research Letters, 45(11), 9275–9287.

[US-SRC] Wolf, S., Keenan, T.F., Fisher, J.B., Baldocchi, D.D., Desai, A.R., Richardson, A.D., Scott, R.L., Law, B.E., Litvak, M.E., Brunsell, N.A., Peters, W., van der Laan-Luijkx, I.T. (2016) Warm spring reduced carbon cycle impact of the 2012 US summer drought, Proceedings of the National Academy of Sciences, 113(21), 5880-5885.

[US-SRM] Barron-Gafford, G. A., Scott, R. L., Jenerette, G. D., Hamerlynck, E. P., Huxman, T. E. (2013) Landscape And Environmental Controls Over Leaf And Ecosystem Carbon Dioxide Fluxes Under Woody Plant Expansion, Journal Of Ecology, 101(6), 1471-1483

[US-UMB] Aron, P. G., Poulsen, C. J., Fiorella, R. P., Matheny, A. M. (2019) Stable Water Isotopes Reveal Effects Of Intermediate Disturbance And Canopy Structure On Forest Water Cycling, Journal Of Geophysical Research: Biogeosciences, 124(10), 2958-2975.

[US-Wi4] Chu, H., Baldocchi, D. D., Poindexter, C., Abraha, M., Desai, A. R., Bohrer, G., Arain, M. A., Griffis, T., Blanken, P. D., OHalloran, T. L., Thomas, R. Q., Zhang, Q., Burns, S. P., Frank, J. M., Christian, D., Brown, S., Black, T. A., Gough, C. M., Law, B. E., Lee, X., Chen, J., Reed, D. E., Massman, W. J., Clark, K., Hatfield, J., Prueger, J., Bracho, R., Baker, J. M., Martin, T. A. (2018) Temporal Dynamics Of Aerodynamic Canopy Height Derived From Eddy Covariance Momentum Flux Data Across North American Flux Networks, Geophysical Research Letters, 45(2), 9275–9287.

References

Ács, F.: A Comparative Analysis of Transpiration and Bare Soil Evaporation, Boundary-Layer Meteorology, 109, 139–162, https://doi.org/10.1023/A:1025473221779, 2003.

Azaele, S., Pigolotti, S., Banavar, J. R., and Maritan, A.: Dynamical Evolution of Ecosystems, Nature, 444, 926–928, https://doi.org/10.1038/nature05320, 2006.

Baldocchi, D., Falge, E., Gu, L., Olson, R., Hollinger, D., Running, S., Anthoni, P., Bernhofer, C., Davis, K., Evans, R., Fuentes, J., Goldstein, A., Katul, G., Law, B., Lee, X., Malhi, Y., Meyers, T., Munger, W., Oechel, W., U, K. T. P., Pilegaard, K., Schmid, H. P., Valentini, R., Verma, S., Vesala, T., Wilson, K., and Wofsy, S.: FLUXNET: A New Tool to Study the Temporal and Spatial Variability of Ecosystem-Scale Carbon Dioxide, Water Vapor, and Energy Flux Densities, Bulletin of the American Meteorological Society, 82, 2415–2434, https://doi.org/10.1175/1520-0477(2001)082<2415:FANTTS>2.3.CO;2, 2001.

Biederman, J. A., Scott, R. L., Goulden, M. L., Vargas, R., Litvak, M. E., Kolb, T. E., Yepez, E. A., Oechel, W. C., Blanken, P. D., Bell, T. W., Garatuza-Payan, J., Maurer, G. E., Dore, S., and Burns, S. P.: Terrestrial Carbon Balance in a Drier World: The Effects of Water Availability in Southwestern North America, Global Change Biology, 22, 1867–1879, https://doi.org/10.1111/gcb.13222, 2016.

Boden, T. A., Krassovski, M., and Yang, B.: The AmeriFlux Data Activity and Data System: An Evolving Collection of Data Management Techniques, Tools, Products and Services, Geoscientific Instrumentation, Methods and Data Systems, 2, 165–176, https://doi.org/10.5194/gi-2-165-2013, 2013.

Briggs, L. J. and Shantz, H. L.: The Water Requirement of Plants, U.S. Government Printing Office, 1913.

Cheng, L., Zhang, L., Wang, Y.-P., Canadell, J. G., Chiew, F. H. S., Beringer, J., Li, L., Miralles, D. G., Piao, S., and Zhang, Y.: Recent Increases in Terrestrial Carbon Uptake at Little Cost to the Water Cycle, Nature Communications, 8, 110, https://doi.org/10.1038/s41467-017-00114-5, 2017.

Chu, H., Christianson, D. S., Cheah, Y. W., Pastorello, G., O'Brien, F., Geden, J., Ngo, S. T., Hollowgrass, R., Leibowitz, K., Beekwilder, N. F., Sandesh, M., Dengel, S., Chan, S. W., Santos, A., Delwiche, K., Yi, K., Buechner, C., Baldocchi, D., Papale, D., Keenan, T. F., Biraud, S. C., Agarwal, D. A., and Torn, M. S.: AmeriFlux BASE Data Pipeline to Support Network Growth and Data Sharing, Scientific Data, 10, 1–13, https://doi.org/10.1038/s41597-023-02531-2, 2023.

Clements, F. E.: Plant Physiology and Ecology, H. Holt, 1907.

Clements, F. E.: Plant Indicators: The Relation of Plant Communities to Process and Practice, Carnegie Institution of Washington, ISBN 978-0-598-34455-7, 1920.

Clements, F. E. and Weaver, J. E.: Experimental Vegetation: The Relation of Climaxes to Climates (Ch. 5), Carnegie Institution of Washington, ISBN 978-0-598-85155-0, 1924.

Currie, P. O. and Peterson, G.: Using Growing-Season Precipitation to Predict Crested Wheatgrass Yields, Journal of Range Management. 19(5): 284-288., 19, 284–288, https://doi.org/10.2307/3895721, 1966.

de Buffon, G.-L. L. C.: Histoire naturelle generale et particuliere, vol. Tome IX, de l'Imprimerie de F. Dufart, 1761.

Dirmeyer, P. A., Zeng, F. J., Ducharne, A., Morrill, J. C., and Koster, R. D.: The Sensitivity of Surface Fluxes to Soil Water Content in Three Land Surface Schemes, Journal of Hydrometeorology, 1, 121–134, https://doi.org/10.1175/1525-7541(2000)001<0121:TSOSFT>2.0.CO;2, 2000.

Eagleson, P. S.: Climate, Soil, and Vegetation: 5. A Derived Distribution of Storm Surface Runoff, Water Resources Research, 14, 741–748, https://doi.org/10.1029/WR014i005p00741, 1978a.

Eagleson, P. S.: Climate, Soil, and Vegetation: 3. A Simplified Model of Soil Moisture Movement in the Liquid Phase, Water Resources Research, 14, 722–730, https://doi.org/10.1029/WR014i005p00722, 1978b.

Eagleson, P. S.: Climate, Soil, and Vegetation: 7. A Derived Distribution of Annual Water Yield, Water Resources Research, 14, 765–776, https://doi.org/10.1029/WR014i005p00765, 1978c.

Eagleson, P. S.: Climate, Soil, and Vegetation: 4. The Expected Value of Annual Evapotranspiration, Water Resources Research, 14, 731–739, https://doi.org/10.1029/WR014i005p00731, 1978d.

Eagleson, P. S.: Climate, Soil, and Vegetation: 6. Dynamics of the Annual Water Balance, Water Resources Research, 14, 749–764, https://doi.org/10.1029/WR014i005p00749, 1978e.

Farrar, T. J.: Vegetation Response to Rainfall and Soil Moisture Variability in Botswana, Ph.D. thesis, Florida State University, 1991.

Feldman, A. F.: The Pulse of Global Vegetation: Do Individual Rainfall Events Create a Lasting Imprint on Photosynthesis?, New Phytologist, https://doi.org/10.1111/nph.70463, 2025.

Feldman, A. F., Short Gianotti, D. J., Konings, A. G., McColl, K. A., Akbar, R., Salvucci, G. D., and Entekhabi, D.: Moisture Pulse-Reserve in the Soil-Plant Continuum Observed across Biomes, Nature Plants, 4, 1026–1033, https://doi.org/10.1038/s41477-018-0304-9, 2018.

Feldman, A. F., Short Gianotti, D. J., Konings, A. G., Gentine, P., and Entekhabi, D.: Patterns of Plant Rehydration and Growth Following Pulses of Soil Moisture Availability, Biogeosciences, 18, 831–847, https://doi.org/10.5194/bg-18-831-2021, 2021.

Forster, J. R.: Observations Made during a Voyage Round the World [in H.M.S. Resolution], G. Robinson, https://doi.org/10.5962/bhl.title.50538, 1778.

Garbulsky, M. F., Peñuelas, J., Papale, D., Ardö, J., Goulden, M. L., Kiely, G., Richardson, A. D., Rotenberg, E., Veenendaal, E. M., and Filella, I.: Patterns and Controls of the Variability of Radiation Use Efficiency and Primary Productivity across Terrestrial Ecosystems, Global Ecology and Biogeography, 19, 253–267, https://doi.org/10.1111/j.1466-8238.2009.00504.x, 2010.

Georg Forster: Ansichten Vom Niederrhein, von Brabant, Flandern, Holland, England Und Frankreich, 1790, 1791.

Goward, S. N. and Prince, S. D.: Transient Effects of Climate on Vegetation Dynamics: Satellite Observations, Journal of Biogeography, 22, 549–564, https://doi.org/10.2307/2845953, 1995.

Green, J. K.: The Intricacies of Vegetation Responses to Changing Moisture Conditions, New Phytologist, 244, 2156–2162, https://doi.org/10.1111/nph.20182, 2024.

Hay-Chapman, F. M. and Dirmeyer, P. A.: A Novel Method for Diagnosing Land–Atmosphere Coupling Sensitivity in a Single-Column Model, Journal of Hydrometeorology, 24, 2207–2223, https://doi.org/10.1175/JHM-D-22-0237.1, 2023.

Holtzman, N., Sloan, B., Potkay, A., Katul, G., Feng, X., and Konings, A. G.: Ecosystem Water-Saving Timescale Varies Spatially With Typical Drydown Length, AGU Advances, 5, e2023AV001 113, https://doi.org/10.1029/2023AV001113, 2024.

Hoorn, C., Ebersbach, J., and Muellner-Riehl, A.: Humboldt, Biogeography, and the Dimension of Time, in: Alexander von Humboldt: Multiperspective Approaches, edited by Falk, G. C., Strecker, M. R., and Schneider, S., pp. 61–95, Springer International Publishing, Cham, ISBN 978-3-030-94008-9, https://doi.org/10.1007/978-3-030-94008-9_3, 2022.

Houerou, H. N. L.: The Rangelands of the Sahel, Journal of Range Management, 33, 41, https://doi.org/10.2307/3898226, 1980.

Hsu, J. S., Powell, J., and Adler, P. B.: Sensitivity of Mean Annual Primary Production to Precipitation, Global Change Biology, 18, 2246–2255, https://doi.org/10.1111/j.1365-2486.2012.02687.x, 2012.

Huang, M., Piao, S., Zeng, Z., Peng, S., Ciais, P., Cheng, L., Mao, J., Poulter, B., Shi, X., Yao, Y., Yang, H., and Wang, Y.: Seasonal Responses of Terrestrial Ecosystem Water-Use Efficiency to Climate Change, Global Change Biology, 22, 2165–2177, https://doi.org/10.1111/gcb.13180, 2016.

Humboldt, A. and Bonpland, A.: Essay on the Geography of Plants (Excerpts), in: Nineteenth-Century Gardens and Gardening, Routledge, 2024.

Hutchings, S. S.: Increasing Forage Yields and Sheep Production on Intermountain Winter Ranges, U.S. Department of Agriculture, 1953.

Huxman, T. E., Smith, M. D., Fay, P. A., Knapp, A. K., Shaw, M. R., Loik, M. E., Smith, S. D., Tissue, D. T., Zak, J. C., Weltzin, J. F., Pockman, W. T., Sala, O. E., Haddad, B. M., Harte, J., Koch, G. W., Schwinning, S., Small, E. E., and Williams, D. G.: Convergence across Biomes to a Common Rain-Use Efficiency, Nature, 429, 651–654, https://doi.org/10.1038/nature02561, 2004.

Jin, Y. and Goulden, M. L.: Ecological Consequences of Variation in Precipitation: Separating Short- versus Long-Term Effects Using Satellite Data, Global Ecology and Biogeography, 23, 358–370, https://doi.org/10.1111/geb.12135, 2014.

Knapp, A. K. and Smith, M. D.: Variation Among Biomes in Temporal Dynamics of Aboveground Primary Production, Science, 291, 481–484, https://doi.org/10.1126/science.291.5503.481, 2001.

Knapp, A. K., Ciais, P., and Smith, M. D.: Reconciling Inconsistencies in Precipitation–Productivity Relationships: Implications for Climate Change, New Phytologist, 214, 41–47, https://doi.org/10.1111/nph.14381, 2017.

Koppen, W. P. and Geiger, R.: Klimakarte Der Erde, Justus Perthes, 1923.

Lambers, H. and Oliveira, R. S.: Plant Water Relations, in: Plant Physiological Ecology, edited by Lambers, H. and Oliveira, R. S., pp. 187–263, Springer International Publishing, Cham, ISBN 978-3-030-29639-1, https://doi.org/10.1007/978-3-030-29639-1_5, 2019.

Lauenroth, W. K.: Grassland Primary Production: North American Grasslands in Perspective, in: Perspectives in Grassland Ecology: Results and Applications of the US/IBP Grassland Biome Study, edited by French, N. R., pp. 3–24, Springer, New York, NY, ISBN 978-1-4612-6182-7, https://doi.org/10.1007/978-1-4612-6182-7_2, 1979.

Lauenroth, W. K. and Sala, O. E.: Long-Term Forage Production of North American Shortgrass Steppe, Ecological Applications, 2, 397–403, https://doi.org/10.2307/1941874, 1992.

Lawes, J. B.: The Average Produce of Wheat, The Gardener's Chronical and Agricultural Gazette, pp. 834–835, 1848a.

Lawes, J. B.: Influence of Climate upon Agriculture, The Gardener's Chronical and Agricultural Gazette, p. 59, 1848b.

Le Houerou, H. N.: Rain Use Efficiency: A Unifying Concept in Arid-Land Ecology, Journal of Arid Environments, 7, 213–247, https://doi.org/10.1016/S0140-1963(18)31362-4, 1984.

Le Houerou, H. N., Bingham, R. L., and Skerbek, W.: Relationship between the Variability of Primary Production and the Variability of Annual Precipitation in World Arid Lands, Journal of Arid Environments, 15, 1–18, https://doi.org/10.1016/S0140-1963(18)31001-2, 1988.

Lieth, H.: Modeling the Primary Productivity of the World, in: Primary Productivity of the Biosphere, edited by Jacobs, J., Lange, O. L., Olson, J. S., Wieser, W., Lieth, H., and Whittaker, R. H., vol. 14, pp. 237–263, Springer Berlin Heidelberg, Berlin, Heidelberg, ISBN 978-3-642-80915-6 978-3-642-80913-2, https://doi.org/10.1007/978-3-642-80913-2_12, 1975.

Livingston, B. E.: The Relation of Desert Plants to Soil Moisture and to Evaporation, Carnegie institution of Washington, 1906.

Maximow, N. A. and Krasnosselsky-Maximow, T. A.: Wilting of Plants in Its Connection with Drought Resistance, Journal of Ecology, 12, 95–110, https://doi.org/10.2307/2255547, 1924.

McColl, K. A., Wang, W., Peng, B., Akbar, R., Short Gianotti, D. J., Lu, H., Pan, M., and Entekhabi, D.: Global Characterization of Surface Soil Moisture Drydowns, Geophysical Research Letters, 44, 3682–3690, https://doi.org/10.1002/2017GL072819, 2017.

Mikhail I Budyko: Klimat I zhizn, Leningrad Gidrometeoizdat Izdatelstvo, Leningrad, USSR, 1971.

Mu, Q., Heinsch, F. A., Zhao, M., and Running, S. W.: Development of a Global Evapotranspiration Algorithm Based on MODIS and Global Meteorology Data, Remote Sensing of Environment, 111, 519–536, https://doi.org/10.1016/j.rse.2007.04.015, 2007.

Mu, Q., Zhao, M., and Running, S. W.: MODIS Global Terrestrial Evapotranspiration (ET) Product (NASA MOD16A2/A3), Algorithm Theoretical Basis Document, Collection, 5, 381–394, 2013.

Nicholson, S. E., Davenport, M. L., and Malo, A. R.: A Comparison of the Vegetation Response to Rainfall in the Sahel and East Africa, Using Normalized Difference Vegetation Index from NOAA AVHRR, Climatic Change, 17, 209–241, https://doi.org/10.1007/BF00138369, 1990.

Novick, K. A., Biederman, J. A., Desai, A. R., Litvak, M. E., Moore, D. J. P., Scott, R. L., and Torn, M. S.: The AmeriFlux Network: A Coalition of the Willing, Agricultural and Forest Meteorology, 249, 444–456, https://doi.org/10.1016/j.agrformet.2017.10.009, 2018.

Noy-Meir, I.: Desert Ecosystems: Environment and Producers, Annual Review of Ecology and Systematics, 4, 25–51, https://doi.org/10.1146/annurev.es.04.110173.000325, 1973.

Paruelo, J. M., Lauenroth, W. K., Burke, I. C., and Sala, O. E.: Grassland Precipitation-Use Efficiency Varies Across a Resource Gradient, Ecosystems, 2, 64–68, https://doi.org/10.1007/s100219900058, 1999.

Pastorello, G., Trotta, C., Canfora, E., Chu, H., Christianson, D., Cheah, Y.-W., Poindexter, C., Chen, J., Elbashandy, A., Humphrey, M., Isaac, P., Polidori, D., Reichstein, M., Ribeca, A., van Ingen, C., Vuichard, N., Zhang, L., Amiro, B., Ammann, C., Arain, M. A., Ardö, J., Arkebauer, T., Arndt, S. K., Arriga, N., Aubinet, M., Aurela, M., Baldocchi, D., Barr, A., Beamesderfer, E., Marchesini, L. B., Bergeron, O., Beringer, J., Bernhofer, C., Berveiller, D., Billesbach, D., Black, T. A., Blanken, P. D., Bohrer, G., Boike, J., Bolstad, P. V., Bonal, D., Bonnefond, J.-M., Bowling, D. R., Bracho, R., Brodeur, J., Brummer, C., Buchmann, N., Burban, B., Burns, S. P., Buysse, P., Cale, P., Cavagna, M., Cellier, P., Chen, S., Chini, I., Christensen, T. R., Cleverly, J., Collalti, A., Consalvo, C., Cook, B. D., Cook, D., Coursolle, C., Cremonese, E., Curtis, P. S., D'Andrea, E., da Rocha, H., Dai, X., Davis, K. J., Cinti, B. D., de Grandcourt, A., Ligne, A. D., De Oliveira, R. C., Delpierre, N., Desai, A. R., Di Bella, C. M., di Tommasi, P., Dolman, H., Domingo, F., Dong, G., Dore, S., Duce, P., Dufrêne, E., Dunn, A., Dušek, J., Eamus, D., Eichelmann, U., ElKhidir, H. A. M., Eugster, W., Ewenz, C. M., Ewers, B., Famulari, D., Fares, S., Feigenwinter, I., Feitz, A., Fensholt, R., Filippa, G., Fischer, M., Frank, J., Galvagno, M., Gharun, M., Gianelle, D., Gielen, B., Gioli, B., Gitelson, A., Goded, I., Goeckede, M., Goldstein, A. H., Gough, C. M., Goulden, M. L., Graf, A., Griebel, A., Gruening, C., Grunwald, T., Hammerle, A., Han, S., Han, X., Hansen, B. U., Hanson, C., Hatakka, J., He, Y., Hehn, M., Heinesch, B., Hinko-Najera, N., Hörtnagl, L., Hutley, L., Ibrom, A., Ikawa, H., Jackowicz-Korczynski, M., Janouš, D., Jans, W., Jassal, R., Jiang, S., Kato, T., Khomik, M., Klatt, J., Knohl, A., Knox, S., Kobayashi, H., Koerber, G., Kolle, O., Kosugi, Y., Kotani, A., Kowalski, A., Kruijt, B., Kurbatova, J., Kutsch, W. L., Kwon, H., Launiainen, S., Laurila, T., Law, B., Leuning, R., Li, Y., Liddell, M., Limousin, J.-M., Lion, M., Liska, A. J., Lohila, A., López-Ballesteros, A., López-Blanco, E., Loubet, B., Loustau, D., Lucas-Moffat, A., Luers, J., Ma, S., Macfarlane, C., Magliulo, V., Maier, R., Mammarella, I., Manca, G., Marcolla, B., Margolis, H. A., Marras, S., Massman, W., Mastepanov, M., Matamala, R., Matthes, J. H., Mazzenga, F., McCaughey, H., McHugh, I., McMillan, A. M. S., Merbold, L., Meyer, W., Meyers, T., Miller, S. D., Minerbi, S., Moderow, U., Monson, R. K., Montagnani, L., Moore, C. E., Moors, E., Moreaux, V., Moureaux, C., Munger, J. W., Nakai, T., Neirynck, J., Nesic, Z., Nicolini, G., Noormets, A., Northwood, M., Nosetto, M., Nouvellon, Y., Novick, K., Oechel, W., Olesen, J. E., Ourcival, J.-M., Papuga, S. A., Parmentier, F.-J., Paul-Limoges, E., Pavelka, M., Peichl, M., Pendall, E., Phillips, R. P., Pilegaard, K., Pirk, N., Posse, G., Powell, T., Prasse, H., Prober, S. M., Rambal, S., Rannik, u., Raz-Yaseef, N., Rebmann, C., Reed, D., de Dios, V. R., Restrepo-Coupe, N., Reverter, B. R., Roland, M., Sabbatini, S., Sachs, T., Saleska, S. R., Sánchez-Cañete, E. P., Sanchez-Mejia, Z. M., Schmid, H. P., Schmidt, M., Schneider, K., Schrader, F., Schroder, I., Scott, R. L., Sedlák, P., Serrano-Ortíz, P., Shao, C., Shi, P., Shironya, I., Siebicke, L., Šigut, L., Silberstein, R., Sirca, C., Spano, D., Steinbrecher, R., Stevens, R. M., Sturtevant, C., Suyker, A., Tagesson, T., Takanashi, S., Tang, Y., Tapper, N., Thom, J., Tomassucci, M., Tuovinen, J.-P., Urbanski, S., Valentini, R., van der Molen, M., van Gorsel, E., van Huissteden, K., Varlagin, A., Verfaillie, J., Vesala, T., Vincke, C., Vitale, D., Vygodskaya, N., Walker, J. P., Walter-Shea, E., Wang, H., Weber, R., Westermann, S., Wille, C., Wofsy, S., Wohlfahrt, G., Wolf, S., Woodgate, W., Li, Y., Zampedri, R., Zhang, J., Zhou, G., Zona, D., Agarwal, D., Biraud, S., Torn, M., and Papale, D.: The FLUXNET2015 Dataset and the ONEFlux Processing Pipeline for Eddy Covariance Data, Scientific Data, 7, 225, https://doi.org/10.1038/s41597-020-0534-3, 2020.

Poyatos, R., Granda, V., Molowny-Horas, R., Mencuccini, M., Steppe, K., and Martínez-Vilalta, J.: SAPFLUXNET: Towards a Global Database of Sap Flow Measurements, Tree Physiology, 36, 1449–1455, https://doi.org/10.1093/treephys/tpw110, 2016.

Reich, E., Guo, J., Peltier, D., Palmquist, E., Samuels-Crow, K., Boone, R., and Ogle, K.: Precipitation Pulse Dynamics Are Not Ubiquitous: A Global Meta-Analysis of Plant and Ecosystem Carbon- and Water-Related Pulse Responses, Global Change Biology, 31, e70 327, https://doi.org/10.1111/gcb.70327, 2025.

Reichstein, M., Bahn, M., Mahecha, M. D., Kattge, J., and Baldocchi, D. D.: Linking Plant and Ecosystem Functional Biogeography, Proceedings of the National Academy of Sciences, 111, 13 697–13 702, https://doi.org/10.1073/pnas.1216065111, 2014.

Rosenzweig, M. L.: Net Primary Productivity of Terrestrial Communities: Prediction from Climatological Data, The American Naturalist, https://doi.org/10.1086/282523, 1968.

Rutherford, MC.: Annual Plant Production-Precipitation Relations in Arid and Semi-Arid Regions, South African Journal of Science, 76, 53–57, 1980.

Sala, O. E., Parton, W. J., Joyce, L. A., and Lauenroth, W. K.: Primary Production of the Central Grassland Region of the United States, Ecology, 69, 40–45, https://doi.org/10.2307/1943158, 1988.

Sala, O. E., Gherardi, L. A., Reichmann, L., Jobbágy, E., and Peters, D.: Legacies of Precipitation Fluctuations on Primary Production: Theory and Data Synthesis, Philosophical Transactions of the Royal Society B: Biological Sciences, 367, 3135–3144, https://doi.org/10.1098/rstb.2011.0347, 2012.

Scott, R. L., Biederman, J. A., Hamerlynck, E. P., and Barron-Gafford, G. A.: The Carbon Balance Pivot Point of Southwestern U.S. Semiarid Ecosystems: Insights from the 21st Century Drought, Journal of Geophysical Research: Biogeosciences, 120, 2612–2624, https://doi.org/10.1002/2015JG003181, 2015.

Sehgal, V., Gaur, N., and Mohanty, B. P.: Global Surface Soil Moisture Drydown Patterns, Water Resources Research, 57, e2020WR027 588, https://doi.org/10.1029/2020WR027588, 2021.

Sellers, P. J., Heiser, M. D., Hall, F. G., Verma, S. B., Desjardins, R. L., Schuepp, P. M., and Ian MacPherson, J.: The Impact of Using Area-Averaged Land Surface Properties —Topography, Vegetation Condition, Soil Wetness—in Calculations of Intermediate Scale (Approximately 10 Km2) Surface-Atmosphere Heat and Moisture Fluxes, Journal of Hydrology, 190, 269–301, https://doi.org/10.1016/S0022-1694(96)03130-7, 1997.

Short Gianotti, D.: Monotone Copula Filter, Zenodo, https://doi.org/10.5281/zenodo.17460263, 2025.

Short Gianotti, D. J. and Entekhabi, D.: Local and General Patterns of Terrestrial Water-Carbon Coupling, Geophysical Research Letters, 51, e2024GL109 625, https://doi.org/10.1029/2024GL109625, 2024.

Short Gianotti, D. J., Rigden, A. J., Salvucci, G. D., and Entekhabi, D.: Satellite and Station Observations Demonstrate Water Availability's Effect on Continental-Scale Evaporative and Photosynthetic Land Surface Dynamics, Water Resources Research, 55, 540–554, https://doi.org/10.1029/2018WR023726, 2019.

Short Gianotti, D. J., Akbar, R., Feldman, A. F., Salvucci, G. D., and Entekhabi, D.: Terrestrial Evaporation and Moisture Drainage in a Warmer Climate, Geophysical Research Letters, 47, e2019GL086 498, https://doi.org/10.1029/2019GL086498, 2020.

Short Gianotti, D. J., McColl, K. A., Feldman, A. F., Xu, X., and Entekhabi, D.: Two Sub-Annual Timescales and Coupling Modes for Terrestrial Water and Carbon Cycles, Global Change Biology, 30, e17 463, https://doi.org/10.1111/gcb.17463, 2024.

Smoliak, S.: Bouteloua Prairie over a 5O-year Period, Smoliak, S. "Influence of climatic conditions on production of Stipa-Bouteloua prairie over a 50-year period." Rangeland Ecology & Management/Journal of Range Management Archives, 39, 100–103, 1986.

Sneva, F. A. and Hyder, D. N.: Estimating Herbage Production on Semiarid Ranges in the Intermountain Region, Journal of Range Management, 15, 88–93, https://doi.org/10.2307/3894868, 1962.

Sun, Y., Piao, S., Huang, M., Ciais, P., Zeng, Z., Cheng, L., Li, X., Zhang, X., Mao, J., Peng, S., Poulter, B., Shi, X., Wang, X., Wang, Y.-P., and Zeng, H.: Global Patterns and Climate Drivers of Water-Use Efficiency in Terrestrial Ecosystems Deduced from Satellite-Based Datasets and Carbon Cycle Models, Global Ecology and Biogeography, 25, 311–323, https://doi.org/10.1111/geb.12411, 2016.

Teuling, A. J., Uijlenhoet, R., Hupet, F., and Troch, P. A.: Impact of Plant Water Uptake Strategy on Soil Moisture and Evapotranspiration Dynamics during Drydown, Geophysical Research Letters, 33, https://doi.org/10.1029/2005GL025019, 2006.

Thornthwaite, C. W.: An Approach toward a Rational Classification of Climate, Geographical Review, 38, 55–94, https://doi.org/10.2307/210739, 1948.

Trugman, A. T., Medvigy, D., Mankin, J. S., and Anderegg, W. R. L.: Soil Moisture Stress as a Major Driver of Carbon Cycle Uncertainty, Geophysical Research Letters, 45, 6495–6503, https://doi.org/10.1029/2018GL078131, 2018.

Unkovich, M., Baldock, J., and Farquharson, R.: Field Measurements of Bare Soil Evaporation and Crop Transpiration, and Transpiration Efficiency, for Rainfed Grain Crops in Australia – A Review, Agricultural Water Management, 205, 72–80, https://doi.org/10.1016/j.agwat.2018.04.016, 2018.

von Humboldt, A.: Ideen zu einer Geographie der Planzen nebst einem Naturgemälde der Tropenländer, F. G. Cotta, 1807.

Walter, H.: Grassland, Savanne Und Busch Der Arideren Teile Afrikas in Ihrer Ökologischen Bedingtheit, Jahresbericht über die Fortschritte der wissenschaftlichen Botanik, 87, 750–860, 1939.

Wang, H., Bassiouni, M., Kang, Y., Rifai, S. W., Gherardi, L. A., Ukkola, A., and Keenan, T. F.: Soil Moisture Buffers the Impact of Precipitation Variability on Ecosystem Productivity, Water Resources Research, 62, e2025WR041 521, https://doi.org/10.1029/2025WR041521, 2026.

Willdenow, K. L., Jackson, M. E., Lizars, D., Stewart, C., Maxwell, H., Stannard, J., and John Reid & Co., b. D.: The Principles of Botany, and of Vegetable Physiology, Edinburgh : Printed at the University Press, for William Blackwood ; [London] : and T. Cadell and W. Davies, London, 1805.

Wladimir Koppen: Die Wärmezonen der Erde, nach der Dauer der heissen, gemässigten und kalten Zeit und nach der Wirkung der Wärme auf die organische Welt betrachtet, Meteorologische Zeitschrift, 1, 215–226, 1884.

Yang, Y., Guan, H., Batelaan, O., McVicar, T. R., Long, D., Piao, S., Liang, W., Liu, B., Jin, Z., and Simmons, C. T.: Contrasting Responses of Water Use Efficiency to Drought across Global Terrestrial Ecosystems, Scientific Reports, 6, 23 284, https://doi.org/10.1038/srep23284, 2016.

Yu, G., Song, X., Wang, Q., Liu, Y., Guan, D., Yan, J., Sun, X., Zhang, L., and Wen, X.: Water-Use Efficiency of Forest Ecosystems in Eastern China and Its Relations to Climatic Variables, New Phytologist, 177, 927–937, https://doi.org/10.1111/j.1469-8137.2007.02316.x, 2008.